DEPOSITS OF THE SANDY BRAIDED SOUTH SASKATCHEWAN RIVER: IMPLICATIONS FOR USING MODERN ANALOGUES TO RECONSTRUCT CHANNEL DIMENSIONS FOR USE IN RESERVOIR CHARACTERISATION

Lunt, I. A.[1], G. H. Sambrook Smith[2*], J. L. Best[3], P. J. Ashworth[4], S. N. Lane[5], and C. J. Simpson[6]

[1]Statoil ASA, Sandsliveien 90, PO Box 7190, N-5020 Bergen, Norway
[2]School of Geography, Earth and Environmental Sciences, University of Birmingham, Edgbaston, Birmingham, B15 2TT, U.K.
[3]Departments of Geology, Geography and Mechanical Science and Engineering and Ven Te Chow Hydrosystems Laboratory, University of Illinois at Urbana-Champaign, 1301 W. Green St., Urbana, Illinois 61801, U.S.A.
[4]Division of Geography, School of the Environment, University of Brighton, Sussex, BN2 4GJ, U.K.
[5]Institut de géographie, Faculté des géosciences et de l'environnement, Université de Lausanne, Lausanne, CH-1015, Switzerland
[6]Fulcrum Graphic Communications Inc., TH2-168, Esplanade Avenue East, North Vancouver, BC V7L 4X8, Canada

*Corresponding author

ABSTRACT

The estimation of fluvial geobody dimensions from core data is a notoriously difficult problem in reservoir modelling. To try and improve such estimates and hence reduce uncertainty in geomodels, data on dunes, unit bars, cross-bar channels and compound bars and their associated deposits are presented from the sand-bed braided South Saskatchewan River, Canada. These data are used to provide a test of models that relate the scale of formative bedforms to the dimensions of the preserved deposits, and therefore an insight into how such deposits may be preserved over geologic time. The preservation of bedform geometry is quantified using a comparison of the alluvial architecture above and below the maximum erosion depth of the modern channel deposits. This comparison shows that there is no significant difference in the mean set thickness of dune cross-strata above and below the basal erosion surface of the contemporary channel, thus suggesting that dimensional relationships between dune deposits and the formative bedform dimensions are likely to be valid from both recent and older deposits.

The data show that estimates of mean bankfull flow depth derived from dune, unit bar and cross-bar channel deposits were all very similar. Thus the use of all these metrics together can provide a useful check that all components and scales of the alluvial architecture have been identified correctly when building reservoir models. The data also highlight a number of practical issues with identifying and applying data relating to cross-strata. For example, the deposits of unit bars were found to be severely truncated in length and width, thus only ~10% of the mean barform length may remain making identification in section difficult. For similar reasons, the deposits of compound bars was found to be especially difficult, and hence estimates of channel depth based on this method may be problematic. Where only core data is available (i.e. there is no outcrop data) it is suggested that formative flow depths are best reconstructed using cross-strata formed by dunes. However, this study found that theoretical

relationships between the distribution of set thicknesses and formative dune height result in slight overestimates of the latter, and hence mean bankfull flow depths derived from these measurements.

This study illustrates that the preservation of cross-strata, and thus the paleohydraulic inferences that can be drawn from them, are a function of the ratio of the size and migration rate of bedforms and the time scale of aggradation and channel migration. These factors must be considered when deciding on appropriate length:thickness ratios for the purposes of object-based modelling.

INTRODUCTION

Depositional models for sandy braided rivers are used frequently to interpret ancient fluvial deposits in core and outcrop, and to simulate the subsurface geometry of fluvial reservoirs using stochastic simulations. Such models of sandy braided fluvial deposits have been based on studies of both modern rivers (e.g. Coleman, 1969; Collinson, 1970; Smith, 1971; Miall, 1977; Cant and Walker, 1978; Blodgett and Stanley, 1980; Bridge et al., 1986; Bristow, 1987,1993a; Jordan and Pryor, 1992; Bridge et al., 1998; Fielding et al., 1999; Skelly et al., 2003; Best et al. 2003: Bridge and Lunt, 2006; Sambrook Smith et al., 2006, 2009; Horn et al., 2012) and outcrops (Smith, 1970; McCabe, 1977; Hazeldine, 1983; Bristow, 1993b; Willis, 1993; Miall and Jones, 2003). However, despite these numerous studies, there is still limited data on thicknesses and lateral extents of differing depositional facies from modern rivers as the extensive datasets that would be required are an expensive and time consuming undertaking (Tye, 2004).

This paucity of information represents a particular weakness in the input to fluvial reservoir models, since the dimensions of all scales of modern surface bar and bedforms should be related to their associated deposits and hence provide a powerful tool for reconstructing the scale of a paleoriver from the dimensions of a range of preserved stratasets. Given this relative paucity of quantitative data from modern rivers, the most advanced and widely-used scaling relationships are thus largely based on experimental work with a particular focus on alluvial dunes (e.g. Paola and Borgman, 1991; Leclair and Bridge, 2001), although such relationships remain to be tested fully in the field (see Leclair, 2011 for notable exception). Additionally, while scaling relationships have been developed for dunes and their stratal sets, less progress has been made for bars (Bridge and Lunt, 2006; Hajek and Heller, 2012).

Herein, we will address these issues and provide an analysis of the South Saskatchewan River, Canada, which is one of the type rivers that has been adopted for facies models of sandy braided rivers (Miall, 1977), and their associated depositional records. The aim of this paper is to focus on establishing scaling relationships between the subsurface deposits and their formative surface morphology. These results add to the relatively small pool of data from modern rivers and aid in constraining the limits of the dimensions of different lithofacies used in object-based reservoir models. This is significant since, as demonstrated by Tye (2004), relatively small changes in the dimensions of sedimentary units used in object-based reservoir models can have a significant impact on the resultant modelled sand body distribution.

Specific objectives of this paper are to: 1) use topographic data to quantify the dimensions of surface morphological features in a sandy braided river i.e. dunes, bars and channel fills; 2) quantify the dimensions and grain size characteristics of the preserved deposits of dunes, bars and channel fills using ground-penetrating radar (GPR) and cores; 3) assess how the geometry of the deposits changes with depth, and specifically above and below the basal erosion surface of the modern channel, and 4) generate quantitative relationships between the formative bedform dimensions and resultant deposits observed in outcrop, core or GPR profiles, in order to ascertain their preservability.

STUDY AREA

This study was undertaken along a 10 km reach of the South Saskatchewan River, near Outlook, Saskatchewan (Fig. 1). Full details of the site have been described previously (see Cant and Walker, 1978, and Sambrook Smith et al. 2005, 2006) and so only a brief summary is provided here. The channel belt is approximately 0.6 km wide, has an average

5

slope of 0.00023 and is incised into Quaternary glacio-fluvial and Cretaceous siliciclastic deposits by up to 30 m. Mean grain size, as measured from 365 sediment samples taken from the river bed, ranges from 0.01 mm to 0.7 mm, which encompasses sediments from silty clays to gravelly sands, with a mean of 0.34 mm.

The South Saskatchewan River was impounded by the Gardiner Dam in 1967, which is 25 km upstream of the study site. Bed elevation surveys at a series of cross-sections have been surveyed since 1964 (Phillips, 2003) and indicate that the river has not experienced any statistically-significant change in mean bed elevation near Outlook since impoundment. However, peak discharge has fallen since 1967 with mean annual peak discharge pre- and post- dam construction being 1536 $m^3 s^{-1}$ and 595 $m^3 s^{-1}$ respectively. The river now has low-suspended sediment concentrations, which allows observation of the river bed using aerial photographs during floods (Lane et al., 2010).

Channels are dominated by dunes (Fig. 2) up to ~0.5 m high. Besides these dunes, the river is also characterised by lobate 'unit' bars (Fig. 2) that have heights equivalent to the channel depth, with typical values up to ~1.5 m. Compound bars, which are defined as comprising two or more unit bars, may be up to ~800 m x 400 m in spatial extent. Cross-bar channels are observed eroding into compound bars, with widths up to 10 m and depths of ~ 0.5 m. Eolian reworking of non-vegetated bar-top surfaces is common and can create both eolian ripples and small barchan dunes, although both of these have a low preservation potential.

METHODS OF DATA COLLECTION

Cores, ground-penetrating radar (GPR) profiles, topographic measurements and grain size samples were collected on compound bars from two different reaches of the study area (Fig. 2).

Subsurface data

Approximately 30 km of GPR data were collected on a rectilinear grid on exposed bar

surfaces (Fig. 2) using a pulseEkko 100 GPR with unshielded 200 MHz antennas. GPR

profiles were spaced 25 and 50 m apart, which allowed the larger scales of stratification

associated with unit bars to be mapped in three dimensions. The vertical resolution of the

GPR profiles is around 0.2 m, and thus it was only used to resolve deposits relating to cross-

bar channels and bars. Those measurements associated with dunes were derived from core

(method described below). GPR data were collected by moving the antennae continuously at

a constant speed and at a fixed separation across the ground, rather than remaining stationary

while the shot was gathered, as this reduced the time of acquisition without loss of data

quality. The acquisition parameters and processing steps are shown in Table 1. The frequency

spectrum of the data was used to determine the cut-offs for dewow and bandpass filters and

the GPR data were not migrated in order to preserve spatial relationships between the

stratasets. The mean radar velocity determined from common mid-point (CMP) profiles was

0.05 ± 0.003 m ns^{-1}.

Topographic surveys

Dune and unit bar heights were quantified using topographic data from: 1) Digital

Elevation Models (DEM) derived from aerial photographs (May 2003, May 2004, September

2004 and August 2005). Full details of the DEM methodology are given in Lane *et al*. (2010);

2) a boat-based echosounder survey (September 2005) and 3) a boat-based GPR survey

(September 2005). The DEMs enabled data to be collected from across the study reach while

the echosounder and GPR surveys provided additional data from the main channels for

another time period and discharge for which no aerial photographs were available. In

September 2005, a bathymetric sonar was used for mapping the bed topography of the main

thalweg where flow depths were greater than ~1 m. At the same time, a boat-based GPR

survey of the shallower sections of the channel was also undertaken using a Sensors &

Software Noggin system with shielded 250 MHz antennae. While there was no penetration

into the subsurface using this GPR approach, the dielectric contrast between the water and

channel bed provided detailed topographic data comparable to that of the echosounder (see

Table 1 for summary). Depths acquired from the sonar and GPR were combined with

positional information using dGPS. Measurements for all three methods were precise to

within 0.01m horizontally and 0.02m vertically, examples of which are illustrated in Fig. 3.

Grain size

365 sediment samples were collected from both exposed and sub-aqueous bar

surfaces using a dredge sampler (Phillips, 2003) in the deepest parts of the channels. Grain

size distributions of dry samples were determined using laser particle size analysis for

sediment less than 2 mm diameter, and by sieving for sediment coarser than 2 mm. The

weight percentage of the coarse fractions was converted to a volume percentage, and

combined with the volume percentage of laser-sampled fractions to determine the overall

grain size distribution.

Cores

Cores were collected using both vibracoring (Smith, 1984) and suction coring (Van de

Meene, 1979; Méndez et al., 2003) methods. The cores were 0.076m in diameter and up to

4.2 m long and did not suffer any compaction. Liquefaction and rodding, in which sediment

is pushed in front of the core pipe, affected some vibracores, but were minor in the suction

cores. Epoxy peels were made of the cores by cutting the cores in half along their length, and

pouring epoxy resin onto the exposed surface. The differential permeability of the sediment

resulted in excellent preservation of the sedimentary structures that were then photographed

and logged.

METHODS OF DATA ANALYSIS

The data reported herein extend the work of Sambrook Smith et al. (2006) by providing

greater detail on the process-product relationship, which has been enabled by the greater

spatial coverage of GPR surveys, more frequent acquisition of imagery and collection of

cores. A more quantitative analysis, over and beyond identification of radar facies, is also

possible using the combination of sequential aerial photographs and cores that provide detail

on the deposits of smaller bedforms (e.g. ripples and dunes) that are below the resolution of

the radar data. The methodology used to analyse the different datasets is described below.

RADAR AND SEDIMENTARY FACIES

As reported in Sambrook Smith et al. (2006), four primary radar facies (see Table 2 for

summary) can be identified within the GPR data from the South Saskatchewan River (Fig.

4d): 1) high-angle reflections (from 6° to angle-of repose), interpreted as large-scale inclined

cross-strata formed by migration of bar margins; 2) discontinuous or undular trough-shaped

reflections, interpreted as medium- and small-scale cross-stratification formed by sinuous

crested dunes; 3) low-angle reflections, $<6^o$, interpreted as small-scale cross-strata formed by

the migration of bedforms below the resolution of the radar, and, 4) reflections of variable dip

angle that are enclosed by a concave reflection, interpreted as cross-bar channel fills or bartop

hollows (Best et al., 2006).

The origin of the radar facies has been determined by comparing the GPR profiles

with the formative bedforms identified from the aerial photographs. This methodology allows

the evolution of the channel to be tracked using the imagery, whilst the DEMs derived from

these images provide data on channel topography through time. For example, during periods

of lower flow (Figs 4b, c) change within the channel is relatively modest, with the migration

of dunes and unit bars within channels and minor changes occurring in the planform of the

compound bar. However, higher flows (Fig. 4a, b) resulted in significant reworking of compound bars and more substantial channel migration. These higher flows resulted in major changes in bed morphology due to the lateral and downstream migration of channels, which led to the erosion of compound bars and formation of new compound bars by amalgamation of dunes and unit bars (Figs 4a,b). The location of new compound bars was determined from either the pre-existing bed topography or the planform channel geometry. The DEM surfaces can then be merged with the GPR profiles and used to identify and highlight the deposits of individual bedforms. For example, the position of unit-bar fronts evident on aerial photographs from 2003 (Fig. 4b) corresponds exactly with the extent of high-angle cross strata seen in the GPR profiles (Fig. 4d, indicated by arrows). Similar radar facies have been observed in other bars in the South Saskatchewan River (Sambrook Smith et al., 2006) and within other rivers (i.e., Best et al., 2003; Bridge and Lunt, 2006; Horn et al., 2012).

Figure 4 also exemplifies the overall alluvial architecture commonly found in sandy braided compound bars. For instance, the compound bar at this location comprises 2 stacked unit bars (labelled A, B in Fig. 4d). In both along-stream and across-stream orientations, the cross-sets formed by unit bars are composed of sub-horizontal reflections that steepen from <6 to around 22 degrees as the cross-set thickness increases in a down-dip direction (see arrows in Fig. 4d). These sets commonly terminate in concave-upward reflections that may represent channel fills, or confluence scours at the downstream end of a compound bar (black box on Fig. 4). This methodology thus permits identification of the explicit links between process and product, and allows: i) confidence in the interpretation of the deposits of other unit bars and cross-bar channels in the radar surveys, and ii) the radar surveys to be categorised comprehensively (see examples shown in Figs 5 and 6).

In contrast to the deposits above the basal erosion surface of the modern channel, those below this surface cannot be linked explicitly with their formative depositional

processes. The modern channel base is defined here by a persistent reflection seen within the radar profiles at an elevation equivalent to the channel depth within the study reach (Figs 4-6). Bed scour did not occur below this surface during a 1- in-40 year flood event in the summer of 2005 (Sambrook Smith et al., 2010). On this basis, it is inferred that this erosion surface is the level down to which the modern channel has scoured. If radar facies (from GPR) and grain size variations (from core) are similar in the deposits above and below this erosion surface, then this provides the best basis for inferring their origins are similar.

Our data clearly show that the radar facies observed above the basal erosion surface of the modern channel are also observed below this level (Fig. 7), and that the sedimentary architecture of these facies is very similar to the deposits above the erosion surface (Figs 4-6). It can thus be inferred that the origin of the deposits below the basal erosion surface of the modern channel is broadly similar to that above it, thus allowing direct comparison between the two datasets in order to examine which parts of the formative bedforms are likely to have been preserved. However, it should be noted that this need not always be the case, for example, Horn et al. (2012) document how discharge has decreased in the Holocene on the Platte River resulting in significant change to the associated alluvial architecture. Based on data from the entire study reach, including cores, the detailed descriptions of the deposits are provided below.

ORIGIN AND SCALE OF DEPOSITS

Dunes

Mean dune height is ~ 0.15 m under low-flow conditions (<100 m^3s^{-1}) and increases to ~0.49 m under high discharges > 600 m^3s^{-1} (Fig. 8a). Dune wavelength displays a weak inverse relationship with discharge, with mean wavelengths of ~12 m under low-flow conditions and ~7.5 m at higher discharges (Fig. 8b). These dune height and wavelength data

suggest that dunes become steeper (i.e. their height:wavelength ratio increases) as discharge increases, as has been shown in past work (e.g. Allen, 1982). Some of the scatter in the relationships between dune size and discharge, especially with respect to dune wavelength, may be due to the use of discharge rather than depth (although there is a strong relationship between discharge and depth on this river; Thomas, 2006). As discussed by Bridge (2003), it is possible to possess contrasting dune geometries even at a constant discharge, with large dunes forming in a channel with low velocity but high depth whereas smaller dunes may form in a channel with high velocity and lower depth. Additionally, the variability in dune morphology may be due to a dune lag effect (see summaries in Allen, 1992; Bridge, 2003), as the dune form takes time to adjust to a new flow depth. Thus it is not uncommon for dune dimensions to be less than equilibrium values during rising stage, but greater during falling stage. Data are not available at a sufficiently-high temporal resolution to investigate these issues further herein.

Many cross-strata formed by dunes are below the resolution of the radar data, and thus the information relating to dunes is largely restricted to that derived from cores (see Reesink and Bridge (2007) for detailed discussion of identifying dunes in core). Above the basal erosion surface, the mean dune set thickness is 0.07 m with a range from 0.01 m to 0.43 m (Fig. 9). Average set thickness below the basal erosion surface is the same as that above it, 0.07 m, but the range of set thicknesses is less (0.01 m – 0.31 m (Fig. 9). Mean thickness of the dune cross-strata is thus ~14 to 47% smaller than the mean bedform height in the modern channels (as compared with dunes measured at high and low discharges, respectively).

Unit bars

The wavelength of unit bars shows a positive relation with discharge, with mean wavelengths of 210 and 606 m in low and higher flow conditions respectively (Fig. 10).

Similarly, the mean height of unit bars measured from echosounder and GPR profiles varied from ~ 0.46 m under low-flow conditions to 1.25 m at high discharges. This trend of an increasing unit bar size with discharge may be expected given flow width is likely a strong control on bar geometry (Yalin, 1992). Figure 11 shows that the ratio of unit-bar wavelength : channel width is constant at a value of ~2 (the channel width herein is defined as the width of individual anabranches, and not the channel-belt width), although the values reported herein are smaller than the ratios of 5-7 suggested by Yalin (1992) and values of between 3 and 12 reported from theoretical, field and experimental data by Lewin (1976), Nelson (1990), Tubino et al. (1999), Lanzoni (2000a,b) and Lunt et al. (2004).

Comparison of cores with GPR data (Figure 12) shows that the low-angle, undulating reflections that make up the majority of the unit bar deposits comprise medium-scale cross-sets formed by dunes. Figure 13 shows the change in the dimensions of unit bar sets above and below the basal erosion surface, as derived from measurements made from the GPR profiles. Above the basal erosion surface, unit-bar deposits vary in length from 10 to 108 m with a mean of 46 m, and in thickness from 0.29 to 1.44 m with a mean of 0.68 m. However, unit-bar deposits below the basal erosion surface are only 6 to 78 m long with a mean of 23 m, and 0.25 to 1.38 m thick with a mean of 0.59 m. This yields length:thickness ratios of simple large-scale sets ranging from ~20 to 143 with a mean of 69 above the basal erosion surface, whereas below the basal erosion surface the range is only ~10 to 80 with a mean of 37. These values above the basal erosion surface are very similar to those reported by Lunt et al. (2004) from a gravel-bed braided river. Important observations to note here are that: 1) the lengths of unit bars are significantly more truncated than their thicknesses; 2) thicknesses below the basal erosion surface are only slightly smaller than those above; 3) the alluvial architecture of unit bar deposits appears the same above and below the erosion surface, comprising large-scale cross-strata that increase in thickness and dip angle in a downstream

direction; and 4) the majority of the unit bar deposits are composed of medium-scale dune cross-sets. Comparison of the dimensions of unit-bar deposits below and above the basal erosion surface, show that they are ~50% shorter below than those above this surface, and are ~10 % of the length of the mean formative bedform. The mean thickness of unit-bar deposits below the basal erosion surface is ~ 87% of unit-bar deposits above this surface. Thus unit bar deposits below the channel base are ~50% as thick as the mean bedform height in the modern channels at high flow, and slightly larger than the mean bedform height at low flow. This clearly indicates that the deposits of unit bars below the basal erosion surface have been more strongly reworked than the younger deposits above this surface, and that this truncation of sets most likely occurs by erosion of the bar margins (i.e. set lengths are only ~10% of formative bedforms) rather than surface erosion of the deposited barform (i.e. set thicknesses are ~50% of high flow formative bedforms).

The vertical trends in grain size of unit-bar deposits above and below the channel base are similar. Data from cores (Fig. 8) shows that unit bar deposits fine upwards, from very coarse or coarse sand to medium sand near the base of the compound bar, and then from medium to fine sand towards the top of the compound bar. This trend agrees well with the surface grain size data (Figure 14) that show the coarsest sediment occurs in the deepest parts of active channels, especially in confluences, and also on the outer bends of channels, and finer sediment is present in the upper parts of the compound bar. Clay deposits are rarely observed in core, and range in thickness from a few millimetres to 0.2 m, and from the GPR profiles appear up to tens of metres in their lateral extent. Observations of the bed surface show that clay deposits are formed in sheltered low-velocity zones, such as bar-tail areas or in the troughs of dunes or unit bars (Sambrook Smith et al., 2006).

Cross-bar channels

Cross-bar channels have an erosional, concave-upward base when viewed in cross-section, however, this same erosion surface is generally flat when viewed parallel to flow (Figs 4-6). Cross-bar channels are up to 100 m long, 20 - 50 m wide and 0.5 - 1.4 m in thickness. Also seen in the GPR profiles are reflections that appear as isolated concave-upward bounding surfaces regardless of orientation. These are not cross-bar channel but bar-top hollows (Best et al., 2006). These concave-upward surfaces are conformable with high-angle, inclined strata on either side of the hollow that are formed by the gradual filling of bar tail areas by accretion of inwardly-migrating bar tails (Ashworth et al., 1996; Best et al., 2006). These bar tail areas are likely to be filled with sands, or with alternating sandy and muddy strata deposited under conditions of variable discharge (i.e., the U-shaped mixed-fill units of Eberth and Miall (1991)), which are then overlain by high-angle cross-strata that dip towards the centre of the hollow.

Channel fills and the fills of confluence scours below the basal erosion surface are up to 1 m thick with an average of 0.5 m (Fig. 15). The thickness of channel fills above the erosion surface is slightly greater, ranging up to 1.3 m with an average of 0.6 m. The thickness of channel fill deposits below the erosion surface is thus ~ 83 % of the thickness of those channel fills above this surface. It is noteworthy that this is a similar level of truncation as described above for the thicknesses of unit bar deposits. Additionally, sub-horizontal cross-sets are also present in deposits below the basal erosion that are *c.* 0.2 m thick and 10 m long, may contain dipping cross-strata and do not terminate in concave upward reflections, analogous to the Facies 2 described by Sambrook Smith et al. (2006; their fig. 3). These sub-horizontal surfaces are interpreted as being deposited by dunes, or low unit bars, that are accreting on the upstream margins of compound bars. Concave-upward reflections with unit-bar deposits dipping towards each other are also present below the modern channel basal

erosion surface in the GPR profiles, and are interpreted to represent bar-top hollows (Best et al., 2006).

Compound bars

Given the large scale of compound bars, the present datasets are not extensive enough to provide sufficient data on their dimensions although some more qualitative observations are presented herein. GPR profiles (Figs 4-6) show that the deposits of compound-bars comprise an amalgamation of unit-bar deposits, which are often dissected by cross-bar channels that were filled with dunes and rippled sands. Thus, along-stream sections through modern compound bars show large-scale, upstream dipping strata (facies 3) at the upstream end (labelled UD in Fig. 5) that are produced by either: a) sets of cross-strata formed by dunes that are too thin to be resolved on the GPR profiles, or b) thin, unit bar deposits that accrete onto the upstream parts of the compound bar. The majority of the compound bar comprises unit-bar deposits and sub-horizontal planar reflections associated with dunes (facies 2), while downstream and lateral sections of the compound bar contain a high proportion of high-angle cross strata (facies 1) associated with unit-bar fronts and lateral accretion of the compound bar.

Cores through recent compound bars show coarse-grained lags at the base of the bar (this is most likely the reflection picked out in the radar profiles) that are overlain by fining-upward cross-sets associated with the unit bar deposits observed on GPR profiles (Fig. 12). The compound bars show an overall fining-upward trend from very coarse/coarse sand to fine sand. Although it is difficult to identify definitive details of the compound-bar deposits below the basal erosion surface, the vertical grain size trends of compound-bar deposits below the basal erosion surface do appear truncated (Fig. 12). Thus the fines observed in the compound bar deposits above the basal erosion surface are commonly eroded and missing from those

from compound bar deposits below this surface. This implies that, in similar depositional environments that undergo truncation of sets, compound bars will be especially difficult to detect in cores where the grain size trends are absent.

This also matches quantitative data on the proportion of facies at different depths, which also shows differences above and below the basal erosion surface (Figure 7). The proportions of Facies 1 and 3 (high-angle reflections and planar reflections respectively) decreases below the basal erosion surface. Similarly, the proportion of Facies 2 (discontinuous reflections) increases below the basal erosion surface. It is reasoned herein that this trend is most likely due to the preferential truncation of the upper (facies 3) and lateral (facies 1) parts of the deposits of compound bars. Additionally, as facies 3 represents finer-grained sediments, this corroborates the observation above from cores noted concerning grain size trends.

DISCUSSION

The dataset generated in the present study allows testing of theoretical relationships between the dimensions of the formative bedforms and their associated cross-strata. To date, such relationships have been developed largely based on laboratory flume experiments, where flow is uniform and steady and the cross-strata are not subject to the degree of reworking that may be present in a natural river channel.

Dunes

The mean thickness of cross-strata formed by dunes was found to be the same above and below the basal erosion surface, and would have been generated by a range of dune sizes. Thus, based on observations of dune height over a range of flow conditions in the modern South Saskatchewan river, the ratio of mean cross-set thickness to mean dune height ranges from 0.14 to 0.47. This range is very similar to that of 0.17 to 0.49 reported by Leclair (2002)

that was based purely on laboratory experimental data. Leclair and Bridge (2001) provide a

relationship for estimating the preserved cross-set thickness, s_m, based on dune height, h:

$$s_m = 1.8\beta \qquad (1)$$

where estimates of β are made by fitting (Fig. 16) a two-parameter gamma function (Eq.2) to

the probability density function (pdf) of dune height (Paola and Borgman, 1991):

$$p(h) = \frac{h^{\alpha-1}e^{\frac{-h}{\beta}}}{\beta^{\alpha}\Gamma^{\alpha}} \qquad (2)$$

in which α is a parameter also estimated from the fit of the gamma function to the data and Γ^{α}

is the standard gamma function (e.g. Ash, 1993). Non-linear, least-squares fitting of Eq. 2 to

the pdf of dune height results in values of α and β of 2.134 and 0.0597 respectively. This

results in a slight over-estimation of cross-set thickness of 0.11 m, compared with a measured

value of 0.07 m. From the perspective of interpreting the rock record, it is of more interest to

establish the likely formative dune heights based on the preserved cross-set thicknesses, and

use this to estimate the flow depth. Fitting the following to the pdf of cross-set thickness,

$p(s)$:

$$p(s) = \frac{ae^{-as}\left(e^{-as} + as - 1\right)}{\left(1 - e^{-as}\right)^2} \qquad (3)$$

where 1/a is the mean value of the exponential tail of the probability density, provides an

estimate of β=0.0446. According to Leclair and Bridge (2001), the mean formative dune

height, h_m, can be estimated from:

$$h_m = 5.3\beta + 0.001\beta^2 \qquad (4),$$

which yields a predicted mean formative dune height of 0.24 m, compared with a measured

mean dune height of 0.13m. Again, the theory overestimates the mean dune height. However,

if a value of β=0.0276 is used (fitting Eq. 3 to the cross-set pdf data, but excluding the 1st

point that relates to the smallest dunes), the predicted formative dune height is reduced to 0.15 m, which is in much better agreement with the observed dune heights.

Using the approach outlined in Bridge and Tye (2000) and Leclair and Bridge (2001), the mean flow depth can be estimated from formative dune height by assuming that the formative flow depth is between 6 and 10 times the dune height. This results in an estimated mean formative flow depth of between 1.42 and 2.36 m. However, bed topography data collected during a 600 m^{3}s^{-1} event in 2005 indicates that the mean flow depth was 1.2 m (maximum flow depths were around 3.7 m), and thus the theory overestimates the mean flow depth slightly. Two important points emerge from this analysis: 1) dune cross-set thickness relates most closely to the distribution of formative dune heights from average flow conditions, and large dunes have a low preservation potential; and 2) it thus follows that estimates of depth should thus also relate to average flow depths. Note that Leclair (2011), based on analysis of dunes in the Mississippi reaches similar conclusions.

The implication of this finding is that applying this theory for reconstructing original bedform dimensions from the cross-strata, which has largely been developed under experimental conditions, appears to result in modest overestimates of both set thickness and dune height. This overestimation may be attributed to several factors present in the field that have been simplified in the laboratory, including the influence of non-uniform flows and bedform hysteresis, the presence of bedform superimposition and the complex three-dimensionality of flow structure in the field. For example, Leclair (2011) suggests that bend curvature may affect the velocity structure within a channel leading to dune geometries that may not match theoretical estimates based solely on estimates of depth.

Unit bars

Large-scale cross sets generated from unit bars can be analysed in a similar way as those of dunes. Using data from below the basal erosion surface, where the mean cross-set thickness

was 0.59 m, and fitting the Paola-Borgman pdf function to this histogram, gives $\beta = 0.3277$. Using Eq. (4), the formative bedform height is then predicted to be 1.74 m, compared with a mean unit bar height during the 2005 event of 1.25 m, and thus provides a slight overestimate. Mean unit bar height should also be broadly equivalent to average flow depth, with mean flow depth being 1.2 m during the 2005 flood with mean unit bar height being 1.25 m. Therefore, similar to the use of dune sets, existing theory for formative mean bar heights would result in a slight overestimation of mean depth at 1.74 m.

Cross-bar channels

Although there is no equivalent theory associated with cross-bar channel deposits, as compared with dunes, it has been suggested that while cross-bar channel fills can cover a wide range of sizes up to that of the main channel, typically, maximum channel fill depths will be a third or a quarter of the maximum bankfull main channel depth (Bridge, 2003). Applying this rule of thumb to the South Saskatchewan data gives the following estimates; based on the maximum thickness of channel fills above (1.3 m) and below (1.0 m) the basal erosion surface yields estimates of maximum bankfull main channel depth of 3.9-5.2 m and 3.0-4.0 m respectively. These figures compare favourably with maximum recorded channel depths of 3.7 m, although given the slight truncation of sets below the basal erosion surface, the estimate from this location is closer to the upper limit whereas the opposite is true for the estimate from above the basal erosion surface. It should be noted that these estimates concern maximum bankfull depth, whilst the dune and unit bar depths cited above were for average bankfull depth. Bridge (2003) suggests that mean bankfull depth is approximately half that of the maximum, thus yielding values of 2.0-2.6 m and 1.5-2.0 m for above and below the basal erosion surface respectively. These estimates are of a similar range to those estimated using the dune and unit bar methods detailed above. These calculations therefore suggest that useful estimates of main channel depths can be established from cross-bar channel fills.

Compound bars

Similar to cross-bar channels, there is no theory to apply to compound bar deposit dimensions, although it has been suggested that on average a compound bar deposit will comprise three to seven unit bars (Bridge and Lunt, 2006). Thus, if these can be identified then this provides an additional means of estimating paleodepth as compound bar thickness will be equivalent to the maximum bankfull channel depth. With sequential aerial imagery and associated GPR data, it can be relatively straightforward to identify the components of a compound bar in a modern river. For instance, Figure 6 shows a compound bar that comprises 2-3 unit bar deposits, which corresponds with the lower end of Bridge and Lunt's (2006) range, which is perhaps to be expected given that this section of the channel was not the deepest within the river. This modern compound bar also most likely sits on top of a truncated compound bar that defines the basal erosion surface (Fig. 6), which itself appears to comprise 2-3 unit bars. While not definitive, at least for the South Saskatchewan it would appear that the number of unit bars that make up a compound bar relates better to the lower range of that suggested by Bridge and Lunt (2006). At the sections studied herein, the channel deposits comprise two truncated compound bars with a maximum of six unit bars within them. Using a unit bar set thickness of 0.59 m (see above), then this would yield a maximum bankfull depth estimate of 3.5 m, which is very close to the measured value of 3.7 m.

The foregoing analysis highlights several important points. 1) Following deposition, dune sets are of such a scale that they either remain intact or are completely eroded, and this results in a similar mean set thickness from modern and preserved dune deposits. 2) In contrast, the sets produced by larger unit bars become more truncated as they are eroded vertically by amalgamation with other unit bars and laterally by main channel erosion. Thus unit bar sets that lie above the basal erosion surface may be thought of as analogous to rivers

where there is a high rate of aggradation and/or low rate of channel migration. Conversely, the unit bar sets preserved below the basal erosion surface may be more typical of low aggradation rates and/or high rate of channel migration. The importance of channel migration in determining the geometry of the deposits is shown by the irregular nature of many of the cross-set boundaries. 3) The rate of channel migration will also largely determine the degree to which the deposits of unit bars are dissected. If channel migration within the channel belt is rapid relative to the local vertical aggradation rate, then the bar deposits would be expected to undergo greater amounts of both vertical and lateral erosion, and therefore be more strongly truncated (Bridge and Lunt, 2006).

At present, there is insufficient data from a sufficiently wide range of rivers with which to develop these ideas further and establish whether different relationships of unit bar cross-set/formative unit bar height may be appropriate for rivers with different rates of aggradation/channel migration. For example, in contrast to the bars quantified here, Hajek and Heller (2012) report bar deposits from the Castlegate Sandstone that are commonly fully preserved. However, scaling relationships appear more robust and widely applicable for dunes, with the caveat that they relate more to average flow conditions and mean dune height. The largest sets associated with dunes at high flow stage appear to have a low preservation potential, as also concluded by Leclair (2011). These findings highlight that the preservation of cross-strata, and the paleohydraulic inferences that can be drawn from them, are a function of the ratio of the spatio-temporal scale of the bedforms (i.e. how large they are and how rapidly they migrate) to the temporal scale of aggradation and channel migration. Where this ratio is high, as exemplified by unit bars, then the original bedform is more likely to become eroded and its original form modified when preserved in the subsurface. Conversely, when this ratio is smaller, then the bedforms become more completely preserved, as is the case for dunes, and thus these may be of greater value in paleohydraulic reconstructions.

APPLICATION TO RESERVOIR MODELLING

The results of this work can be used to improve scaling relationships in subsurface studies as applied to the prediction of fluvial heterogeneity. The dimensions (length, width and height) of geobodies are defined statistically in stochastic models. Correct recognition of the formative channel depth allows the different scales of heterogeneity in fluvial deposits to be estimated with a reduced uncertainty. We illustrate below how our results can be applied to geobody estimation using data from preserved deposits in this study.

One of the key requirements for reservoir models is an estimate of channel-belt width as this has such a fundamental control on the connectedness of sandstone bodies. Typically as channel-belt width increases then sandstone body connectivity would also be expected to increase. As presented above, estimates of mean formative flow depths from our preserved dune, unit-bar and channel fill measurements are 1.42-2.36 m, 1.74 m and 1.5-2.0 m respectively. Taking the mean of these estimates results in a mean formative flow depth of 1.8 m, which is slightly higher than our measured mean bankfull flow depth of 1.2 m. However, by using the 3 different datasets, the accuracy of the estimation has been increased in comparison with use of any single dataset. An additional point is that our work and recent research by Leclair (2011) both suggest that preserved dunes will relate more to average conditions i.e. mean and not maximum bankfull flow depth. This is important as estimates of channel-belt width using empirical equations are based on mean bankfull flow depth. For example, using the estimate of 1.8 m for mean bankfull flow depth (d_m) and an empirical equation from Bridge and Mackey (1993):

$$cbw = 192d_m^{1.37} \tag{6}$$

channel-belt width (cbw) is estimated to be 430 m as compared with measured values of ~600 m. However, if the estimate of 1.8 m was assumed to relate to maximum bankfull flow

depth then d_m would be assumed to be only 0.9 m (i.e. half the maximum value) resulting in an estimate of *cbw* of only 166 m.

As well as improving estimates of the overall channel-belt sandstone scale the data presented here can also provide important detail for modelling at the within channel scale. Using the estimates of preserved vs. original bedform dimensions, the lateral dimensions of fluvial geobodies can be predicted. Porosity and permeability variations on the scale of dune cross-sets are unlikely to be of much concern at the reservoir scale. However, high-permeability streaks associated with coarse lags at the base of unit bar deposits may have a huge impact on reservoir drainage. Similarly, mud-rich drapes often found at bartail locations will act to reduce vertical and lateral connectivity (e.g. termed 'interbar muds' by Lynds and Hajek, 2006). Therefore, prediction of geobodies on the length-scale of unit-bars is important. Lynds and Hajek (2006) list four channel-scale fine-grained lithofacies (channel-lining muds, interbar muds, inclined heterolithic muds and mud plugs) that can all occur in sandy braided rivers. They demonstrate how estimates of the size of these lithofacies can be derived from estimates of flow depth to better constrain mudstone dimensions used in reservoir models.

Our study has also allowed us to estimate the degree of preservation of bars, which together with the estimate of flow depth can assist with improving estimates of geobody dimensions, an example of which is outlined below. Unit bar deposits scale with formative flow width (see above) and generally have lengths of between 3 and 7 times the channel width. Using typical ranges of flow depth to channel width of 1:200 (Bridge, 2003), the formative channel width is estimated as ~300 m, which implies unit bar lengths of 900 to 2100 m and widths of around 300 m. Using the preservation potential of ~10% found in this study, preserved geobody dimensions would be 30-210 m with a mean around 90 m. Allowing for intersection of high permeability basal lags between 2 or 3 adjacent unit bars (Ramanthayan et al., 2011) this thus gives the potential for high permeability thief zones to

impact reservoir drainage between wells spaced 300 m to 600 m apart. Clearly, identifying the degree of truncation is important in such calculations and our use of 10% preservation may represent a lower limit more typical of low aggradational settings. Conversely, at the other end of the scale bars may be much more fully preserved (e.g. as reported by Hajek and Heller, 2012).

The aim of this example is to demonstrate how detailed analysis reduces the uncertainty in estimates of formative mean flow depths through prediction from preserved dune, unit bar and channel fill deposit thicknesses. The estimation of formative mean flow depth is then used with documented scaling relationships to predict the range of bedform and channel widths. Information on the preservation potential of these bedform widths and lengths from this study are then used to predict the scale of heterogeneities in subsurface fluvial reservoirs with much greater rigour than simple application of dimensional databases. The value of developing scaling relationships is that they are independent of analogue data and allow prediction in any subsurface reservoir with well-described core data.

CONCLUSIONS

This study has described and analysed the morphology and geometry of bedforms and channels in a sandy braided river, and the deposits they produce. This analysis reveals six practical points concerning the use of the preserved alluvial architecture to establish the likely scale of the alluvial channel the sediments were deposited in:

1)   Mean dune cross-set thickness is the same above and below the basal erosion surface. However, large dune cross-sets are not well represented in the subsurface sedimentology, and result in relationships between set thickness, dune height and depth that are more appropriate to *mean bankfull flow depth*. Past theory of formative dune height has been largely tested

with experimental data and appears to overestimate slightly the mean dune height, and hence estimates of flow depth derived from this.

2)   The mean thickness of unit-bar deposits above and below the basal erosion surface is broadly similar. Mean thicknesses below the surface (0.59 m) are ~ 87% of that from those above the basal erosion surface (0.68 m). Thus unit bar deposits below the channel base are ~50% as thick as the mean formative bedform height (as compared with high flow barforms). However, there is a substantial difference in unit bar lengths, which appear to be preferentially truncated as opposed to thickness. Unit-bar deposits below the base of the modern channel are only ~50% as long as those above, and ~10% as long as the formative mean bedform wavelength. Similar to the analysis conducted with dunes, unit bar sets provide a reasonable estimate of mean bankfull flow depth, although a slight overestimate.

3)   The choice of unit bar length:thickness ratio used in object-based models must take into account the extent of unit bar reworking as affected by aggradation rate, the rate of lateral channel migration, variability of bedform dimensions, and intrinsic channel scour. However, the precise nature of these relationships remains unquantified. Thus, existing theory applied to dune cross-strata provides a more robust method for estimating mean flow depth than using the dimensions of unit bar sets. This is especially the case when using core where identifying and interpreting the deposits of unit bars is problematic.

4)   Similar to unit bars, the maximum thickness of the fills of cross-bar channels is only slightly lower below the basal erosion surface than above it

(83%). Given this similarity, using either yields a reasonable estimate of main channel flow depth based on the assumption that the main channel is 3-4 times as deep as the maximum thickness of the cross-bar channel fills. However, this provides an estimate of the maximum bankfull depth. In order to compare this estimate with the methods concerning dunes and unit bars, which relate to mean bankfull depth, then the assumption should be made that this is approximately half the maximum bankfull depth.

5) When taken together, estimates of mean bankfull flow depth obtained from dunes cross-sets (1.89 m), unit bars (1.74 m) and cross-bar channels (1.75 m) are all very similar, but slight overestimates of the measured value (1.2 m). However, given the inherent variability within rivers, these estimates are sufficiently reliable to gain a satisfactory estimate of the overall scale of the alluvial channel. The important point here is that obtaining estimates from a range of different methods should be adopted if possible, as this allows confidence in the use of such estimates. If the estimates from these different methods showed a wide spread, it would suggest that the different scales and features of dunes, unit bars and cross-bar channels had perhaps been identified incorrectly.

6) Individual compound bars can be difficult to identify unequivocally in outcrop and core, and thus provide the least robust method for attempting to establish paleochannel dimensions. In the present study, compound bars above the basal erosion surface (and hence channel depth) were more readily identified based on the presence of more complete fining-up successions within the deposits. However, these compound bars only comprised up to three unit bars. In contrast, the deposits of compound bars

below the basal erosion surface have truncated vertical trends in grain size with their upper fine-grained caps frequently absent, thus making them much more difficult to identify.

While estimates of paleo-channel dimensions can be derived from both core and outcrop, the dimensions of bars and channel fills will vary depending on the degree of truncation and are especially difficult to identify in core alone. Taking all this evidence into account, it is suggested that if only core is available then dune cross-sets provide the most robust method for estimating paleochannel mean bankfull flow depth and hence establishing the overall size of the river. It is, of course, preferable to have outcrop as well as core data so that a range of estimates can be better constrained. The data presented herein suggests correct identification of the different components of the alluvial channel should yield comparable estimates for mean bankfull flow depth. These data demonstrate that when using length and thickness estimates from modern channels to build an object-based reservoir model, consideration of the aggradational history is vital. Herein, we have used a simple split between those deposits above and below the modern channel basal erosion surface to illustrate this point. For example, rapid channel migration relative to the aggradation rate will lead to greater truncation and thus may be more analogous to data from below the basal erosion surface. Clearly, development of these ideas requires the types of measurement provided herein but from a broader range of rivers and depositional history.

REFERENCES

Allen, J. R. L., 1982, Sedimentary Structures: Their Character and Physical Basis: Elsevier, Amsterdam.

Ash, C., 1993, The probability tutoring book, IEEE Press, 480 p.

Ashworth, P. J., J. L. Best, J. Peakall, and J. A. Lorsong, 1999, The influence of aggradation rate on braided alluvial architecture: field study and physical scale-modelling of the Ashburton River gravels, Canterbury Plains, New Zealand, in Smith, N.D. and J. Rogers, eds., Fluvial Sedimentology VI: IAS Special Publication 28, p. 11-50.

Ashworth, P. J., G. H. Sambrook Smith, J.L. Best, J. S. Bridge, S. N. Lane, I. A. Lunt, A. J. H. Reesink, C. J. Simpson, and R. E. Thomas, 2011, Evolution and sedimentology of a channel fill in the sandy braided South Saskatchewan River and its comparison to the deposits of an adjacent compound bar: Sedimentology, v. 58, p. 1860-1883.

Best, J. L., J. Woodward, P. J. Ashworth, G. H. Sambrook Smith, and C. J. Simpson, 2006, Bar-top hollows: a new element in the architecture of sandy braided rivers: Sedimentary Geology, v. 190, p. 241-255.

Blodgett, R. H., and K. O. Stanley, 1980, Stratification, bedforms and discharge relations of the Platte braided river system, Nebraska: Journal of Sedimentary Petrology, v. 50, p. 139-148.

Bridge, J. S., N. D. Smith, F. Trent, S. L. Gabel, and P. Bernstein, P., 1986, Sedimentology and morphology of a low-sinuosity river: Calamus River, Nebraska Sand Hills: Sedimentology, v. 33, p. 851-870.

Bridge, J. S., R. E. L. Collier, and J. Alexander, 1998, Large-scale structure of Calamus river deposits revealed using ground-penetrating radar: Sedimentology, v. 45, p. 977-985.

Bridge, J. S., and I. A. Lunt, 2006, Depositional models of braided rivers, in Sambrook Smith, G. H., J. L. Best, C. S. Bristow, and G. E. Petts, eds., Braided Rivers; process, deposits, ecology and management: IAS Special Publication 36, p. 11-50.

Bridge, J. S., and S. D. Mackey, 1993, A theoretical study of fluvial sandstone body dimensions, in Flint, S. S., and I. D. Bryant, eds., Geological modeling of hydrocarbon reservoirs: IAS Special Publication 15, p. 213-236.

Bridge, J. S., 2003, Rivers and Floodplains: Forms, Processes and Sedimentary Record: Blackwell, Malden, USA, 491 p.

Bridge, J. S., and R. S. Tye, 2000, Interpreting the dimensions of ancient fluvial channel bars, channels, and channel belts from wireline-logs and cores: AAPG Bulletin, v. 84, p. 1205-1228.

Bristow, C. S., 1987, Brahmaputra River: channel migration and deposition, in Ethridge, F. G., R. M. Flores, and M. D. Harvey, eds., Recent Developments in Fluvial Sedimentology: SEPM Special Publication 39, p. 63-74.

Bristow, C. S., 1993a, Sedimentary structures exposed in bar tops in the Brahmaputra River, Bangladesh, in Best, J. L., and C. S. Bristow, eds., Braided Rivers: Geological Society of London Special Publication 75, p. 277-289.

Bristow, C. S. (1993b) Sedimentology of the Rough Rock; a Carboniferous braided river sheet sandstone in northern England, in Best, J. L., and C. S. Bristow, eds., Braided Rivers: Geological Society of London Special Publication 75, p. 291-304.

Cant, D. J., and R. G. Walker, 1978, Fluvial processes and facies sequences in the sandy braided South Saskatchewan River, Canada: Sedimentology, v. 25, p. 625-648.

Coleman, J. M., 1969, Brahmaputra River: Channel processes and sedimentation: Sedimentary Geology, v. 3, p. 129-239.

Collinson, J. D., 1970, Bedforms of the Tana River, Norway: Geografiska Annaler, v. 52A, p. 31-56.

Eberth, D. A., and A. D. Miall, 1991, Stratigraphy, sedimentology and evolution of a vertebrate-bearing braided to anastomosed fluvial system, Cutler Formation (Permian-Pennsylvanian), north-central New Mexico: Sedimentary Geology, v. 72, p. 225-252.

Fielding, C.R., J. Alexander, and R. McDonald, 1999, Sedimentary facies from GPR surveys of the modern, upper Burdekin River of north Queensland, Australia: Consequences of extreme discharge fluctuations, in N. D. Smith, and J. Rogers, eds., Fluvial Sedimentology VI: IAS Special Publication 28, p. 347-362.

Hajek, E.A., and P.L. Heller, 2012, Flow-depth scaling in alluvial architecture and nonmarine sequence stratigraphy: example from the Castlegate Sandstone, central Utah, U.S.A.: Journal of Sedimentary Research, v. 82, p. 121-130.

Hazeldine, R. S., 1983, Fluvial bars reconstructed from a deep, straight channel, Upper Carboniferous coalfield of Northeast England: Journal of Sedimentary Petrology, v. 53, p. 1233-1247.

Horn, J.D., C.R. Fielding, and R.M. Joeckel, 2012, Revision of Platte River alluvial facies model through observations of extant channels and barforms, and subsurface alluvial valley fills: Journal of Sedimentary Research, v. 82, p. 72-91.

Jordan, D. W., and W. A. Pryor, 1992, Hierarchical levels of heterogeneity in a Mississippi River meander belt and application to reservoir systems: AAPG Bulletin, v. 76, p. 1601-1624.

Lane, S. N., P. E. Widdison, R. E. Thomas, P. J. Ashworth, J. L. Best, I. A. Lunt, G. H. Sambrook Smith, and C. J. Simpson, C.J., 2010, Quantification of braided river channel change using archival digital image analysis: Earth Surface Processes and Landforms, v. 35, p. 971-985.

Lanzoni, S., 2000a, Experiments on bar formation in a straight flume 1. Uniform sediment: Water Resources Research, v. 36, p. 3337-3349.

Lanzoni, S., 2000b, Experiments on bar formation in a straight flume 2. Graded sediment: Water Resources Research, v. 36, p. 3351-3363.

Leclair, S. F., and J. S. Bridge, 2001, Quantitative interpretation of sedimentary structures formed by river dunes: Journal of Sedimentary Research, v. 71, p. 713-716.

Leclair, S. F., 2002, Preservation of cross-strata due to the migration of subaqueous dunes: an experimental investigation: Sedimentology, v. 49, p. 1157-1180.

Leclair, S.F., 2011, Interpreting fluvial hydromorphology from the rock record: large-river peak flows leave no clear signature, in S. K. Davidson, S. Leleu, and C. P. North, eds., From River To Rock Record: The Preservation Of Fluvial Sediments And Their Subsequent Interpretation: SEPM Special Publication No. 97, p. 113-123.

Lewin, J., 1976, Initiation of bed forms and meanders in coarse-grained sediment: Geological Society of America Bulletin, v. 87, p. 281-285.

Lunt, I. A., J. S. Bridge, and R. S. Tye, 2004, A quantitative, three–dimensional depositional model of gravelly braided rivers: Sedimentology, v. 51, p. 377-414.

Lynds, R., and Hajek, E., 2006, Conceptual model for predicting mudstone dimensions in sandy braided-river reservoirs: AAPG Bulletin, v. 90, p. 1273-1288.

McCabe, P. J., 1977, Deep distributary channels and giant bedforms in the Upper Carboniferous of the Central Pennines, northern England: Sedimentology, v. 24, p. 271-290.

Méndez, G., M. Pérez-Arlucea, E. Stouthamer, and H. Berendsen, 2003, The TESS-1 suction corer: a new device to extract wet, uncompacted sediments: Journal of Sedimentary Research, v. 73, p. 1078-1081.

Miall, A. D., 1977, A review of the braided river depositional environment: Earth Science Reviews, v. 13, p. 1-62.

Miall, A. D., and B. G. Jones, 2003, Fluvial architecture of the Hawkesbury Sandstone (Triassic), near Sydney, Australia: Journal of Sedimentary Research, v. 73, p. 531-545.

Nelson, J. M., 1990, The initial instability and finite-amplitude stability of alternate bars in straight channels: Earth Science Reviews, v. 29, p. 97-115.

Paola, C., and L. Borgman, 1991, Reconstructing random topography from preserved stratification: Sedimentology, v. 38, p. 553-565.

Phillips, R. T. J., 2003, Downstream geomorphic impacts of reservoir construction on the sand-bed braided South Saskatchewan River, Saskatchewan. Unpublished B.Sc. (Hons) thesis, Simon Fraser University, British Columbia, Canada, 75 pp.

Reesink, A. J. H., and J. S. Bridge, 2007, Influence of superimposed bedforms and flow unsteadiness on formation of cross strata in dunes and unit bars: Sedimentary Geology, v. 202, 281-296.

Sambrook Smith, G. H., P. J. Ashworth, J. L. Best, J. Woodward, and C. J. Simpson, 2005, The morphology and facies of sandy braided rivers: some considerations of scale invariance, inn Blum, M. D., S. B. Marriott, and S. F. Leclair, eds., Fluvial Sedimentology VII: International Association of Sedimentologists Special Publication 35, p. 145-158.

Sambrook Smith, G. H., P. J. Ashworth, J. L. Best, J. Woodward, J., and C. J. Simpson, 2006, The alluvial architecture and sedimentology of the sandy, braided South Saskatchewan River, Canada: Sedimentology, v. 53, p. 413-434.

Sambrook Smith, G. H., P. J. Ashworth, J. L. Best, I. A. Lunt, O. Orfeo, and D. R. Parsons, 2009, The sedimentology and alluvial architecture of a large braid bar, Río Paraná, Argentina: Journal of Sedimentary Research, v. 79, p. 629-642.

Sambrook Smith, G. H., J. L. Best, P. J. Ashworth, S. N. Lane, N. O. Parker, I. A. Lunt, R. E. Thomas, and C. J. Simpson, 2010, Can we distinguish flood frequency and magnitude in the sedimentological record of rivers?: Geology, v. 38, p. 579-582.

Skelly, R.L., C. S. Bristow, and F. G. Ethridge, 2003, Architecture of channel-belt deposits in an aggrading shallow sandbed braided river: the lower Niobrara River, northeast Nebraska: Sedimentary Geology, v. 158, p. 249-270.

Smith, D. G., 1984, Vibracoring fluvial and deltaic sediments – tips on improving penetration and recovery: Journal of Sedimentary Petrology, v. 54, p. 660-663.

Smith, N. D., 1970, The braided stream depositional environment: Comparison of the Platte River with some Silurian clastic rocks, North-Central Appalachians: Bulletin of the Geological Society of America, v. 81, p. 2993-3014.

Smith, N. D., 1971, Transverse bars and braiding in the Lower Platte River, Nebraska: Bulletin of the Geological Society of America, v. 82, p. 3407-3420.

Tubino, M., R. Repetto, and G. Zolezzi, 1999, Free bars in rivers: Journal of Hydraulic Research, v. 37, p. 759-775.

Tye, R. S., 2004, Geomorphology: An approach to determining subsurface reservoir dimensions: AAPG Bulletin, v. 88, p. 1123-1147.

Van de Meene, E. A., J. Van der Staay, and Teoh Lay Hock, 1979, The Van der Staay suctioncorer: a simple apparatus for drilling in sand below groundwater table: Haarlem, The Netherlands, Rijks Geologische Dienst, 24 p.

Willis, B. J., 1993, Ancient river systems in the Himalayan foredeep, Chinji village area, northern Pakistan: Sedimentary Geology, v. 88, p. 1-76.

Yalin, M. S., 1992, River Mechanics: Pergamon Press, 219 p.

TABLES

Bartop GPR profiles				
Acquisition parameters			Processing steps	
Frequency	200 MHz		High-pass filter	20 MHz
Antenna separation	0.75 m		Bandpass filter	21-40-150-300
Shot spacing	0.1 m		Set time-zero	Airwave peak
Sampling interval	0.4 ns		AGC gain function	10 ns window
Stacks	16		Static correction	From GPS data
In-channel GPR profiles				
Acquisition parameters			Processing steps	
Frequency	225 MHz		Trace interpolation	
Antenna separation	0.5 m		High-pass filter	20 MHz
Shot spacing	0.1 m		Bandpass filter	21-40-150-300
Sampling interval	0.4 ns		Set time-zero	Airwave peak
Stacks	16		AGC gain function	10 ns window
			Static correction	From GPS data
			Split-step migration	Using 2-region velocity model

Table 1. Acquisition parameters and processing steps for GPR profiles.
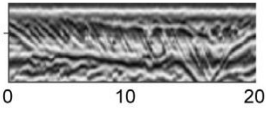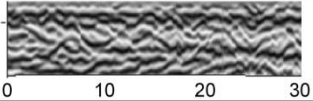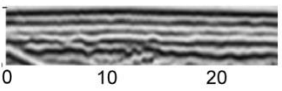
GPR reflection (scale in metres)	Reflection type	Location	Formation
	Facies 1. High angle inclined Angle of dip from 6° to angle of repose. Commonly truncated at top and bottom by sub horizontal reflections	Active bar margin	Flow causes sediment transport over bar migration into channel thalweg
	Facies 2. Discontinuous undular or trough shaped reflections	Channel thalweg	Product of large sinuous crested dune migration in channel thalwegs
	Facies 3. Low angle reflections (< 6°). Can be arranged in sets that dip up/downstream laterally/horizontally	Bar surface	Accretion surfaces on which dunes of a low amplitude are migrating over, or unit bar migration over bar surface
	Facies 4. Reflections of variable dip enclosed by concave reflection	Channel	Filling of channel scours and cross bar channels by unit bars (angle-of-repose) or dunes (low angle or undular)

Table 2: Summary of primary characteristics of radar facies used in this study
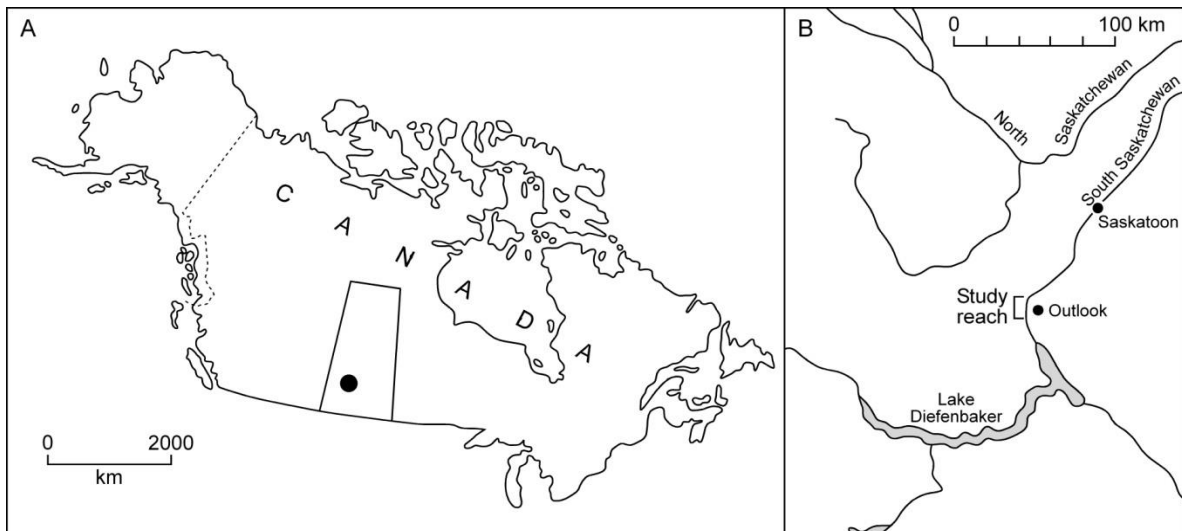
Figure 1: a) Location of Outlook, Saskatchewan, Canada; b) Location of study site on South Saskatchewan River, near Outlook.
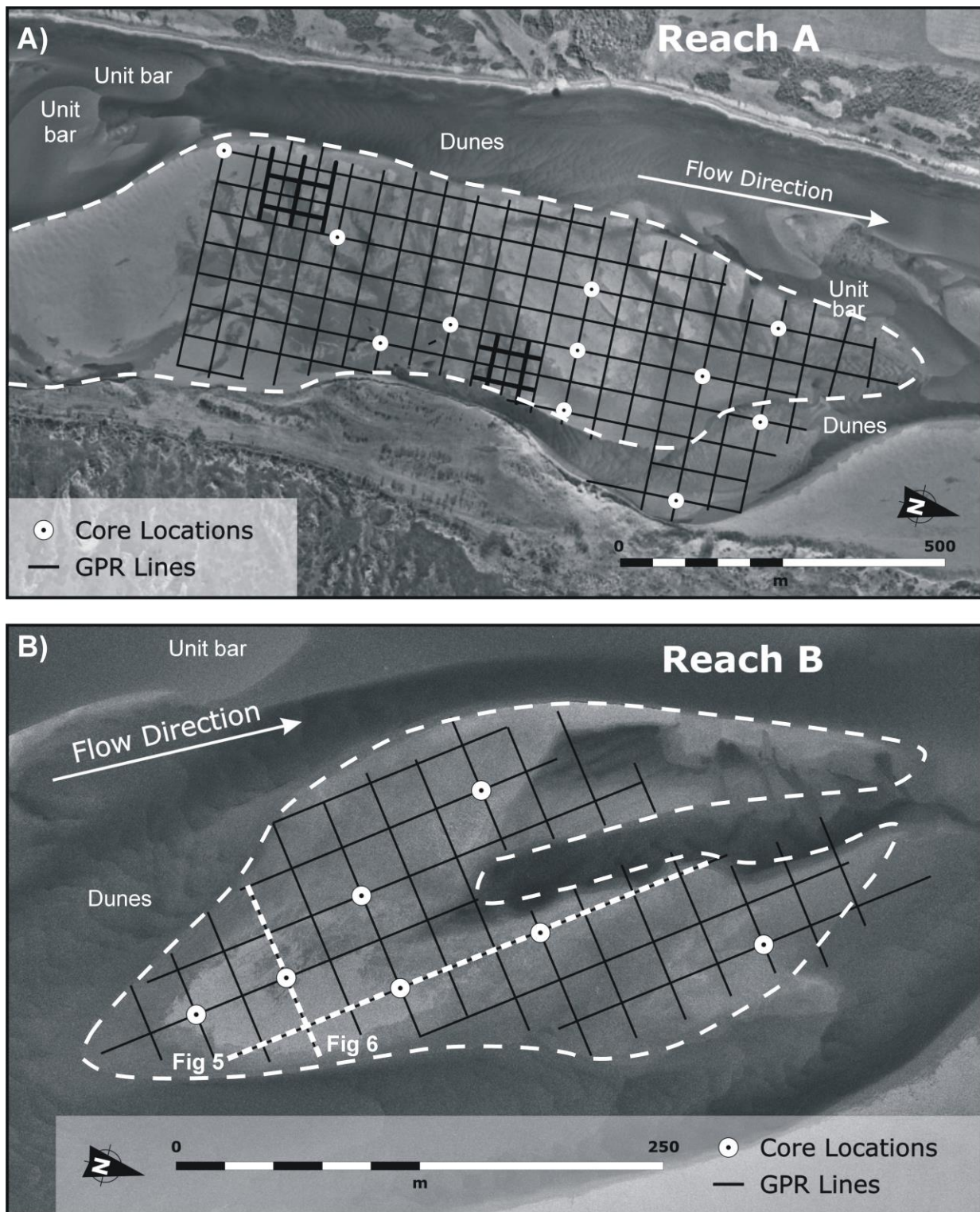
Fig. 2; Aerial photographs of the two primary study areas used in this study showing dunes, unit bars and compound bars in the South Saskatchewan River. Also shown are the GPR survey lines and core locations from which the analysis discussed in the text was derived. Locations of radar data shown in Figs. 5 and 6 are also shown
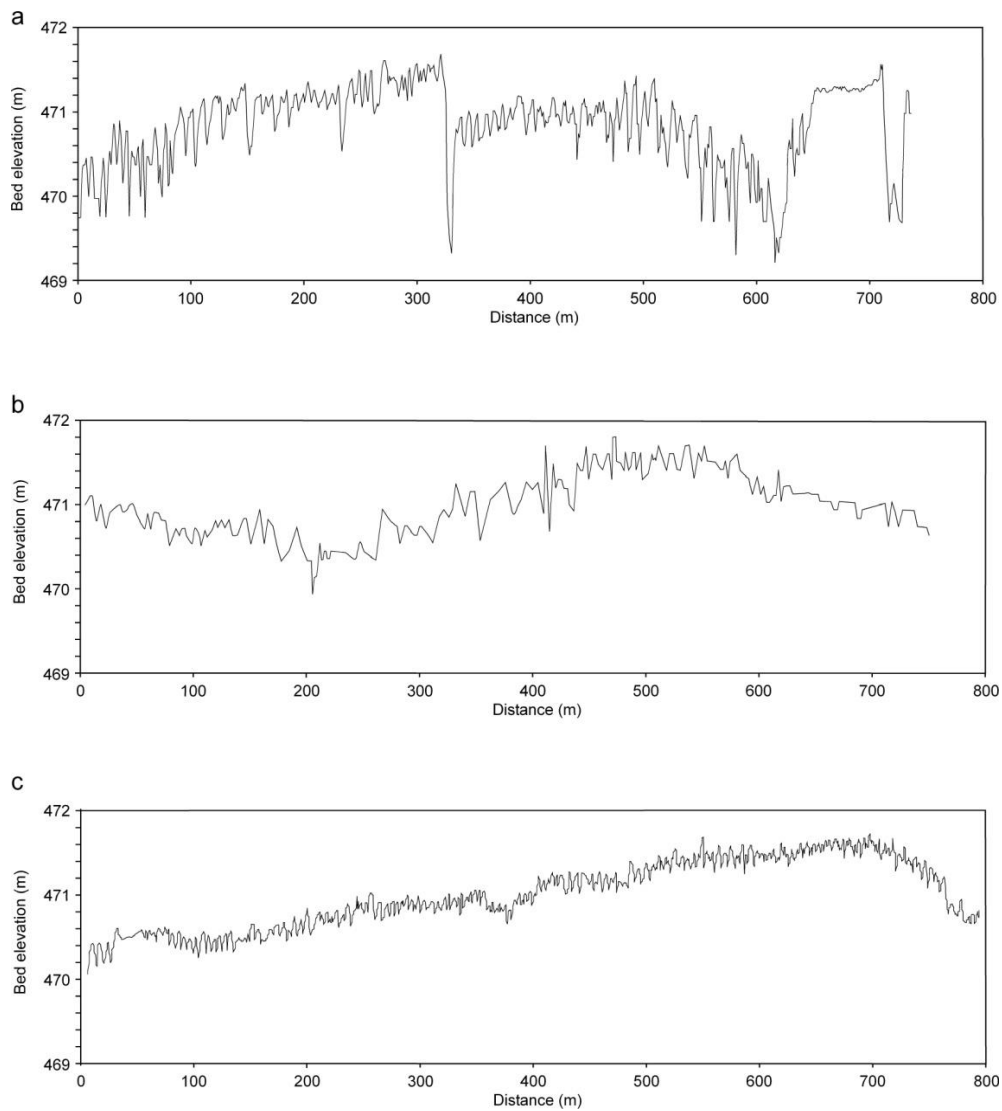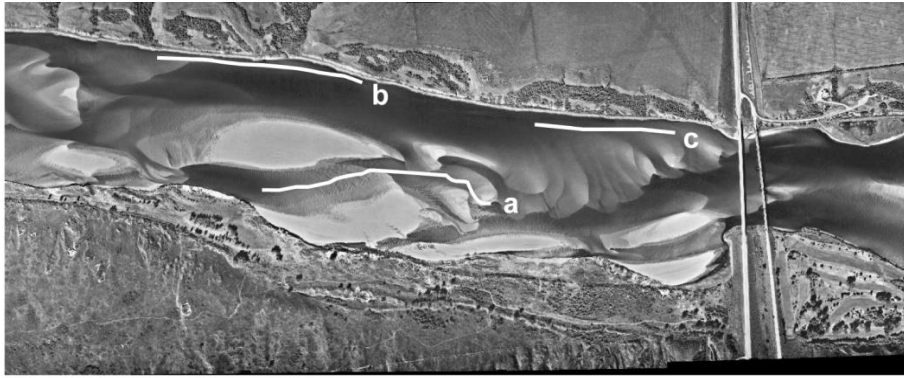
Fig. 3; Examples of topographic data used in the study as derived from: a) DEMs b) echosounder and c) boat-based GPR surveys. Photograph shows the locations of each of the survey lines.
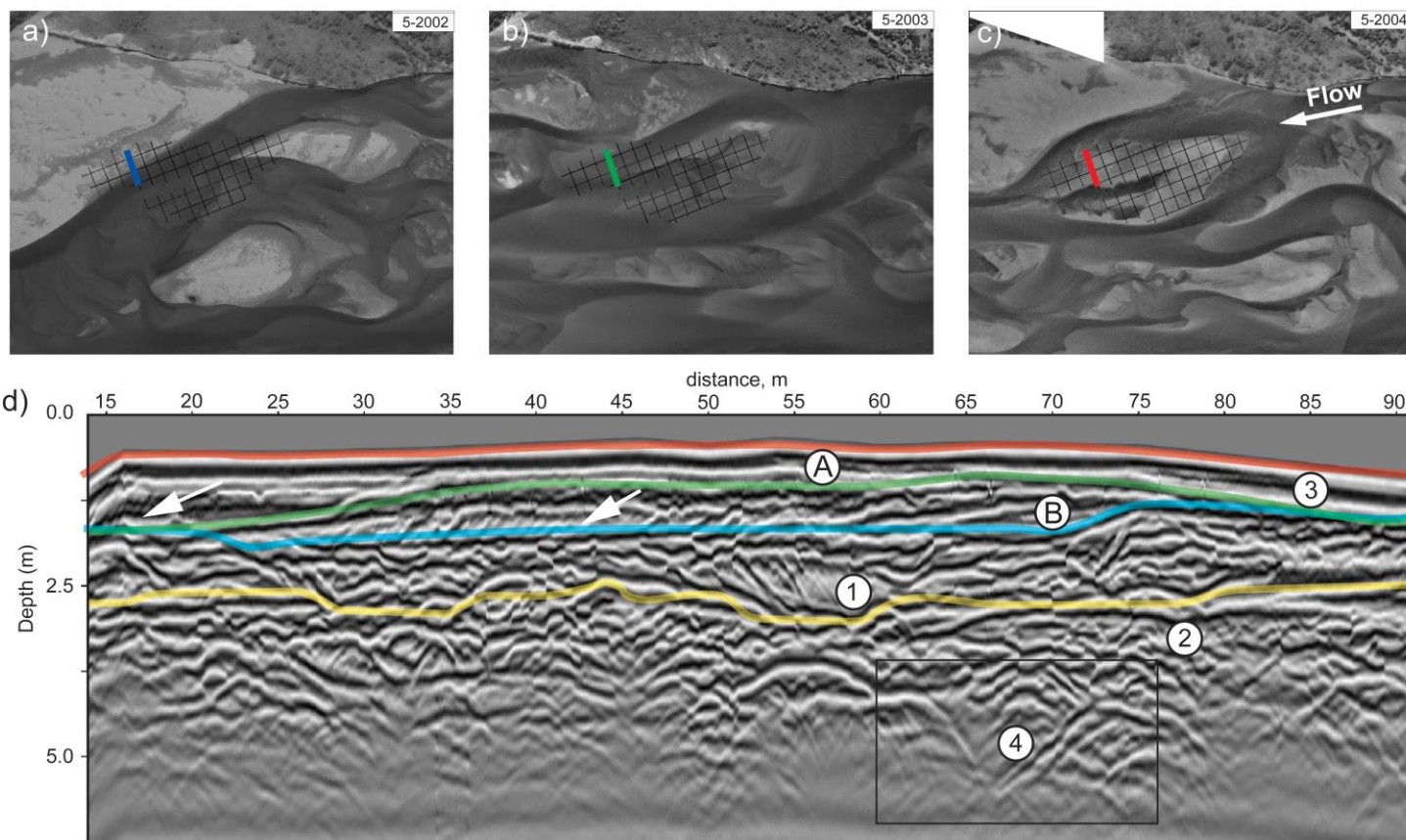
Figure 4: Sequence of aerial photographs showing the location of the GPR profile and the change in bed topography of Reach B between: a) 2002, b) 2003 and c) 2004. d) Radar profile taken in 2004 as indicated by red line in c). The green and blue lines represent the bar surface in 2003 and 2002 respectively with locations of the radar line relative to the channel configuration at those times shown in a) and b). The basal erosion surface of the modern channel at this location is denoted by the yellow line. Representative examples of the radar facies are indicated by numbers. The labels A and B refer to the most recent unit bars that have been deposited at this site: note how they thicken in a downstream direction (flow right to left in all panels) as indicated by the arrows.

Figure 5: Example to illustrate how the radar profiles are interpreted for later quantitiative analysis, see Fig. 2 for location. This profile, taken in an along-stream orientation with flow left to right, shows the main unit bar (green) and cross-bar channel fill (brown) deposits. UD = upstream dipping surfaces. Coloured lines are bar surface in 2004 (red), 2003 (green), 2002 (blue) and the basal erosion surface of the modern channel at this location (yellow).
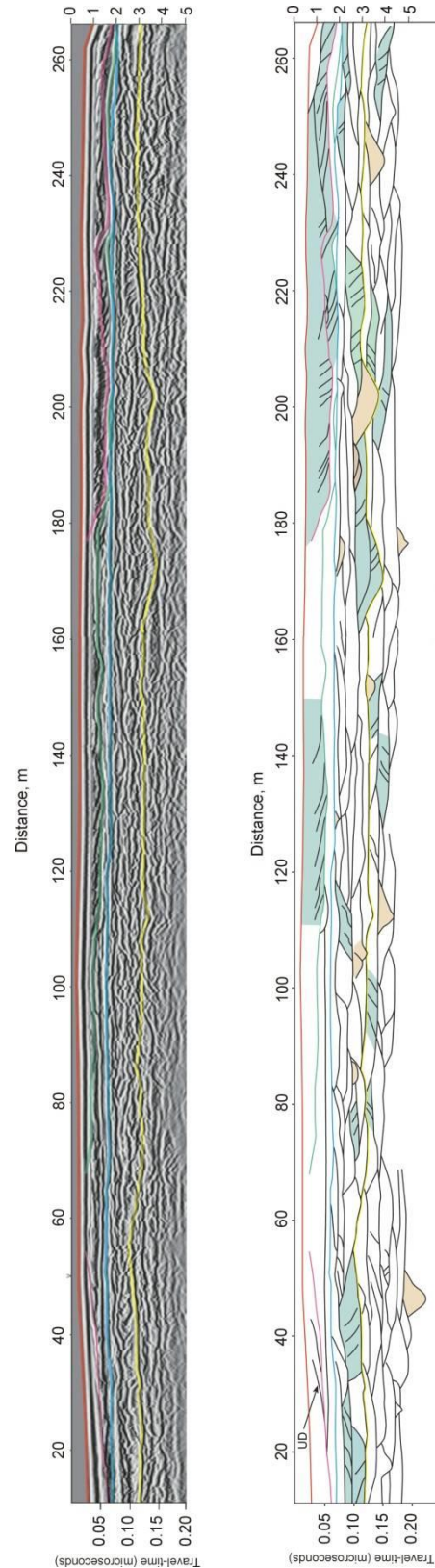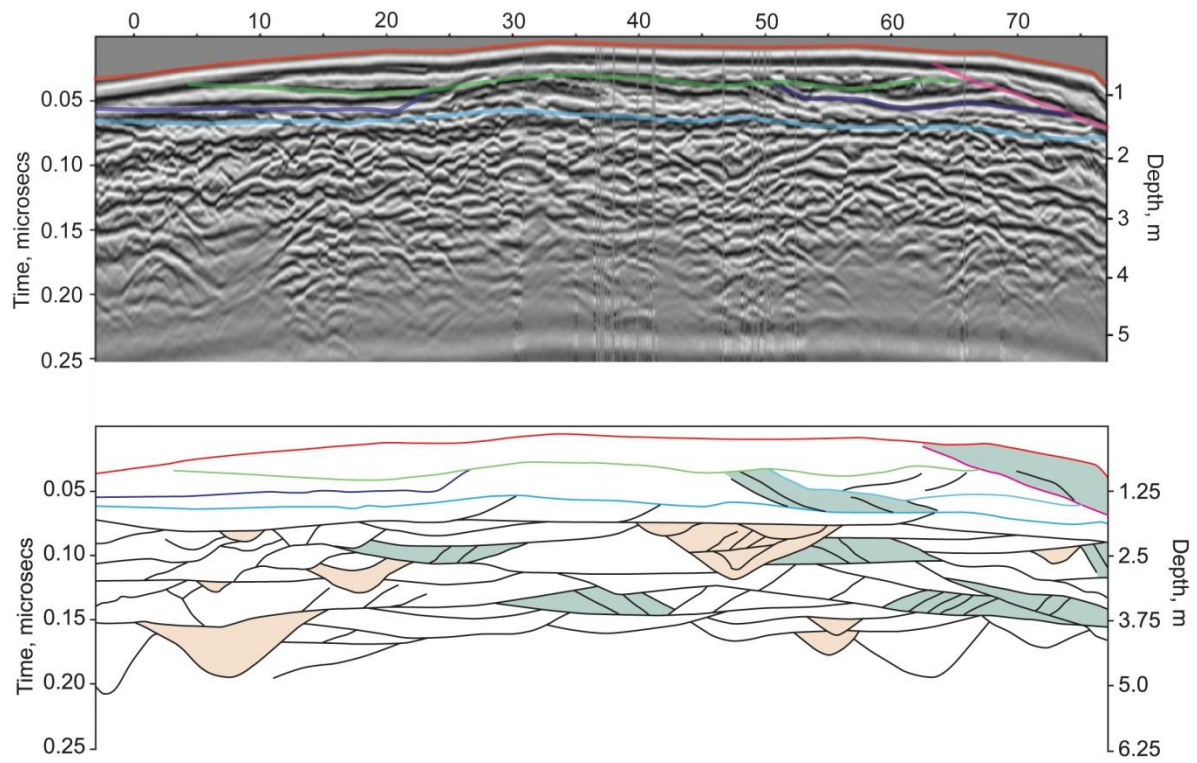
Figure 6: Example to illustrate how the radar profiles are interpreted for later quantitative analysis, see Fig. 2 for location. This profile, taken in a cross-stream orientation, shows the main unit bar (green) and cross-bar (brown) channel fill deposits. Coloured lines are bar surface in 2004 (red), 2003 (green), 2002 (blue) and
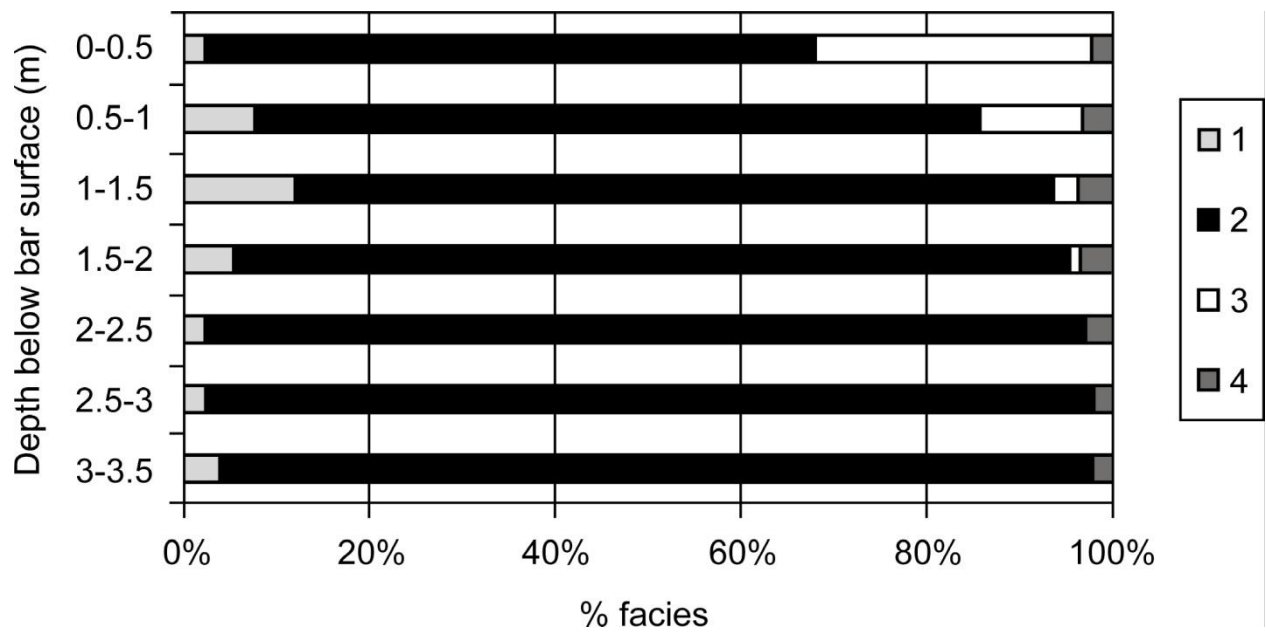
Figure 7: Percentage of radar facies with depth in the deposits. The proportion of facies 1 and 3 below the basal erosion surface are much smaller than those above. The basal erosion surface varies in elevation but is generally at ~3 m depth. Facies 1 is high angle inclined reflections, facies 2 is discontinuous undular or trough shaped reflections, facies 3 is low angle reflections and facies 4 is reflections of variable dip enclosed by a concave reflection (see Table 2).
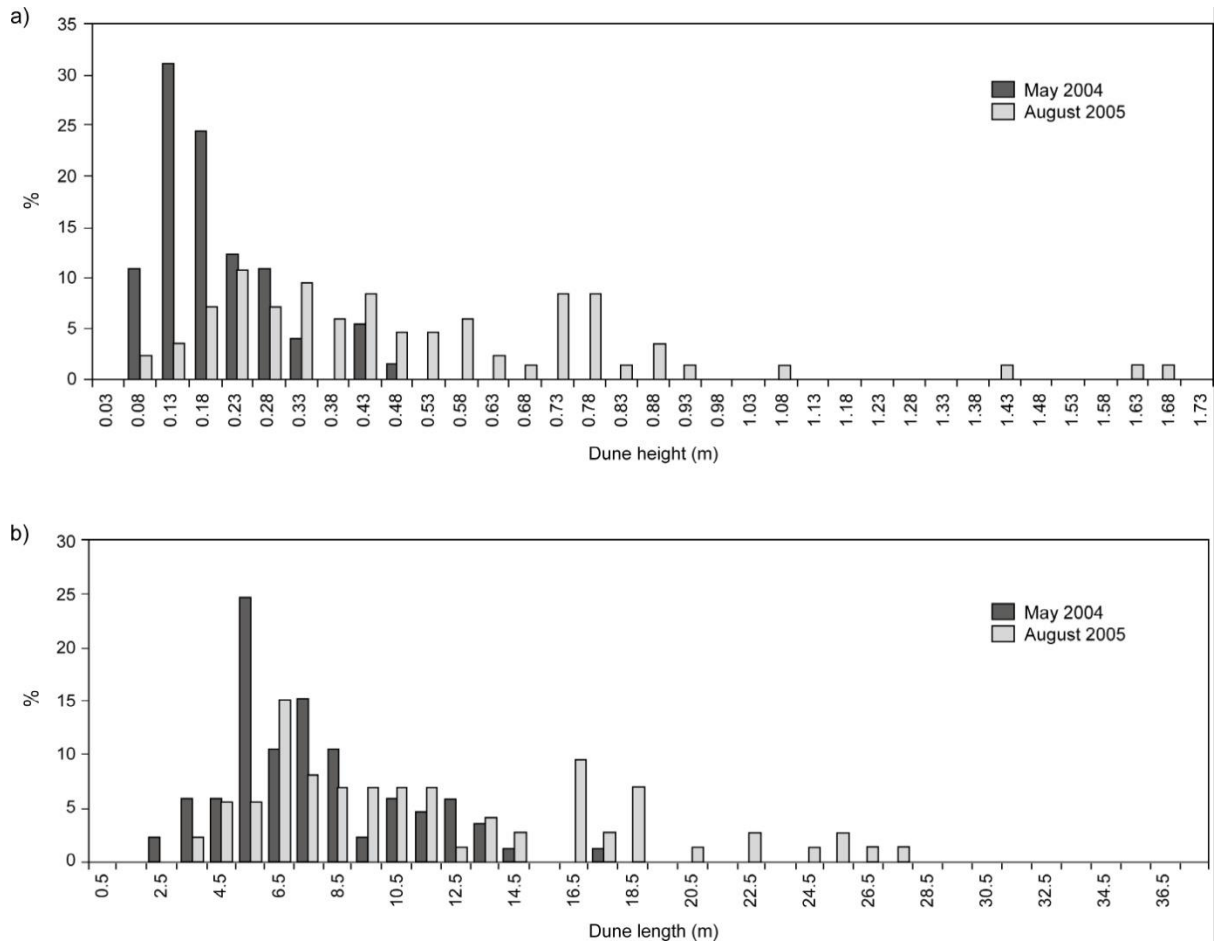
Figure 8: a) dune heights measured for May 2004 (Q ~ 61 m^{3}s^{-1}) and August 2005 (Q ~ 600 m^{3}s^{-1}) b) dune wavelengths as measured for the same periods as above. For 2004 n=74 and for 2005 n=85.
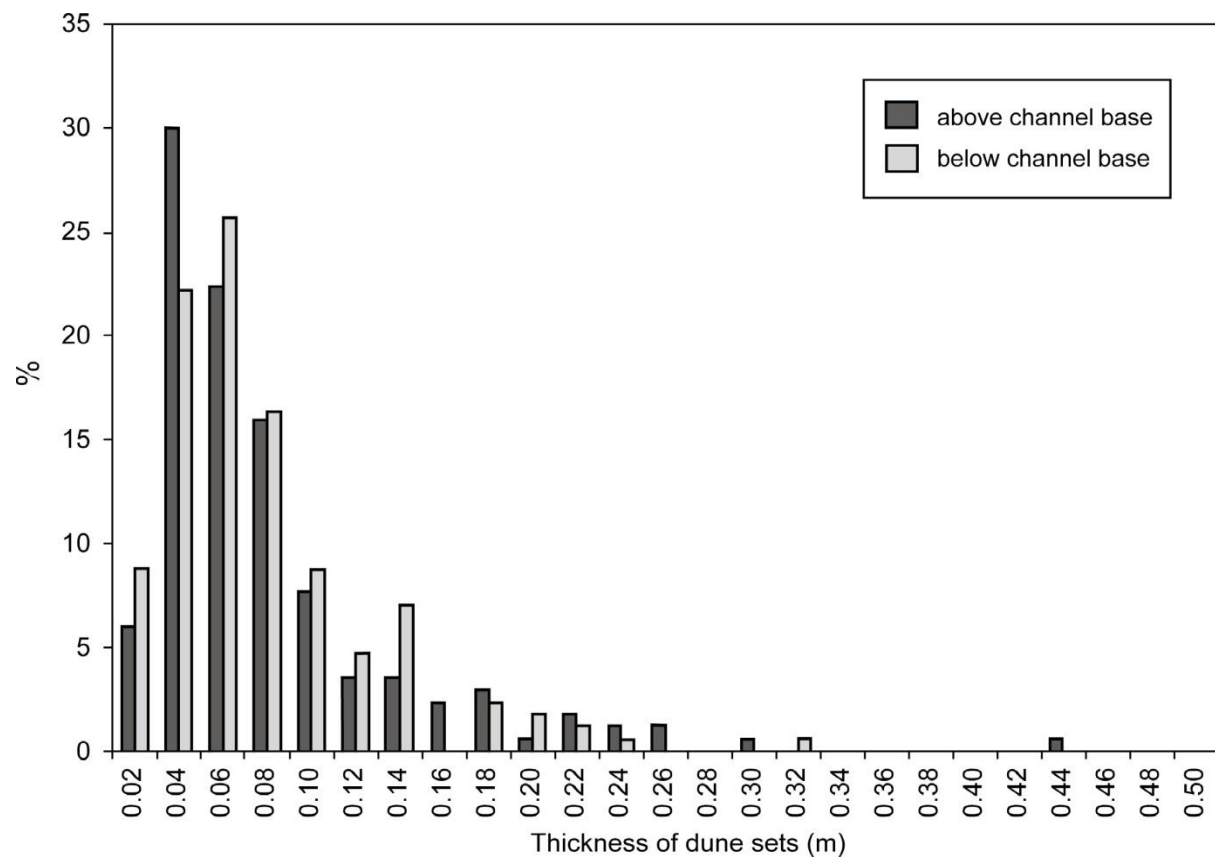
Figure 9: Thickness of medium-scale cross-sets associated with dune deposits as measured from sections of core above (n=170) and below (n=171) the channel basal erosion surface.
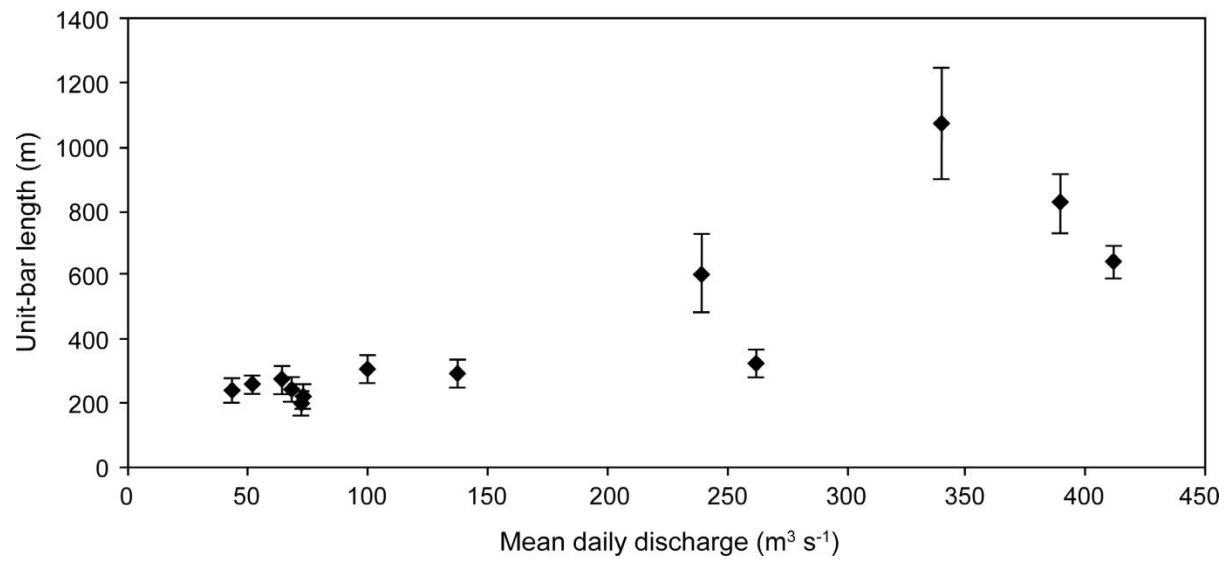
Figure 10: Unit bar length (n=622) as measured from aerial photographs for a range of discharges.
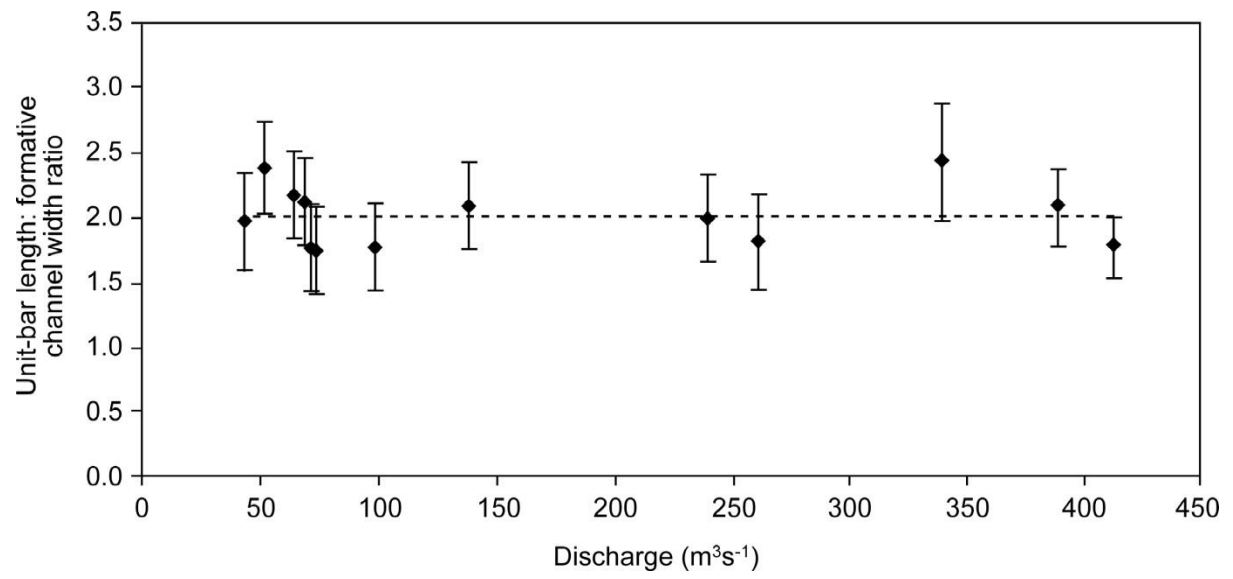
Figure 11: Ratio of mean unit bar length: formative channel width (n=622) shows that bar dimensions scale with flow discharge.

Figure 12: Example of integration of radar and core data, with yellow line indicating the basal erosion surface at this location. The core at this location shows a compound bar with an overall fining-up trend. The compound bar itself comprises three unit bars that also display fining-up trends (labelled FU). Also shown is the truncation of the bar immediately beneath the erosion surface which has no fine-grained surface, in contrast to that above.
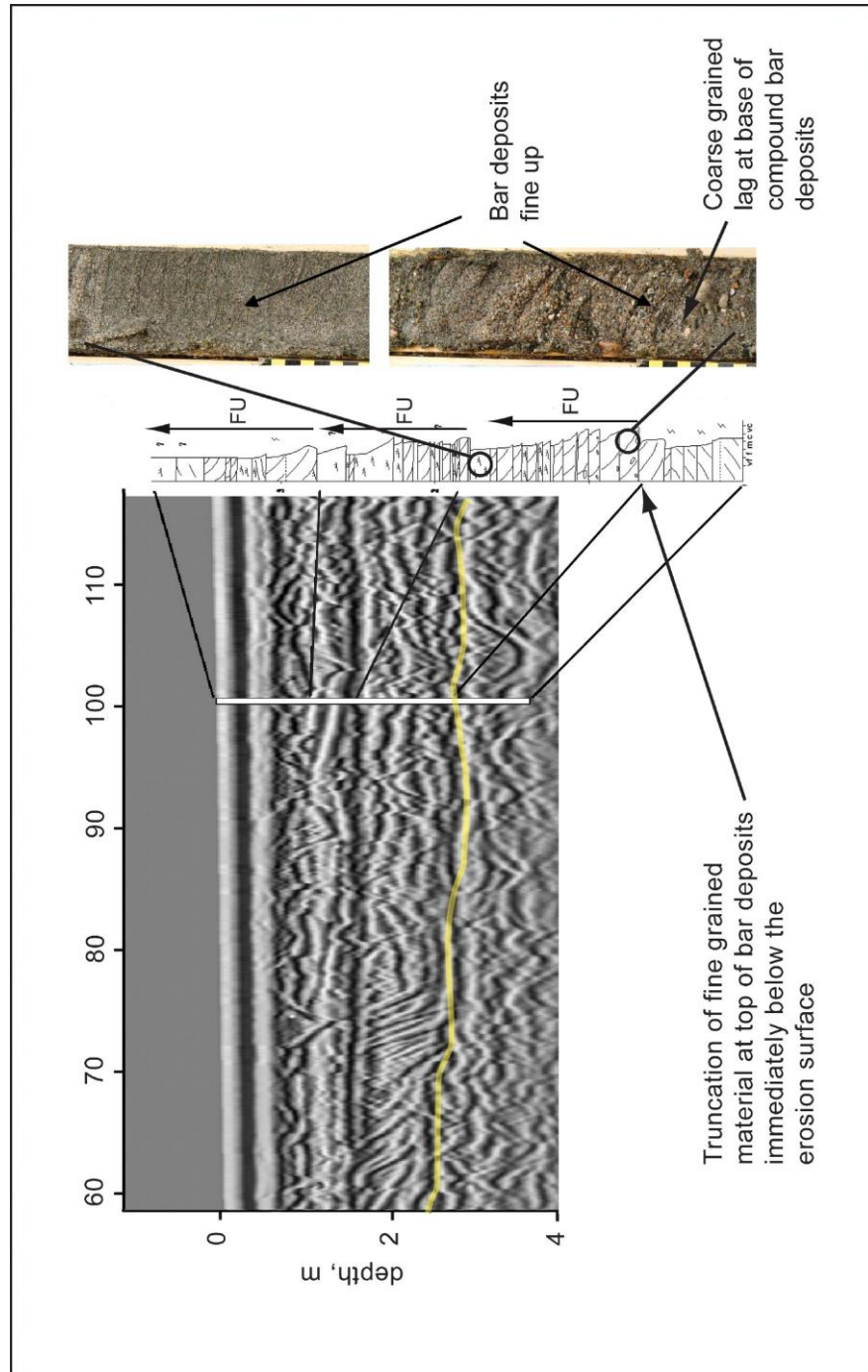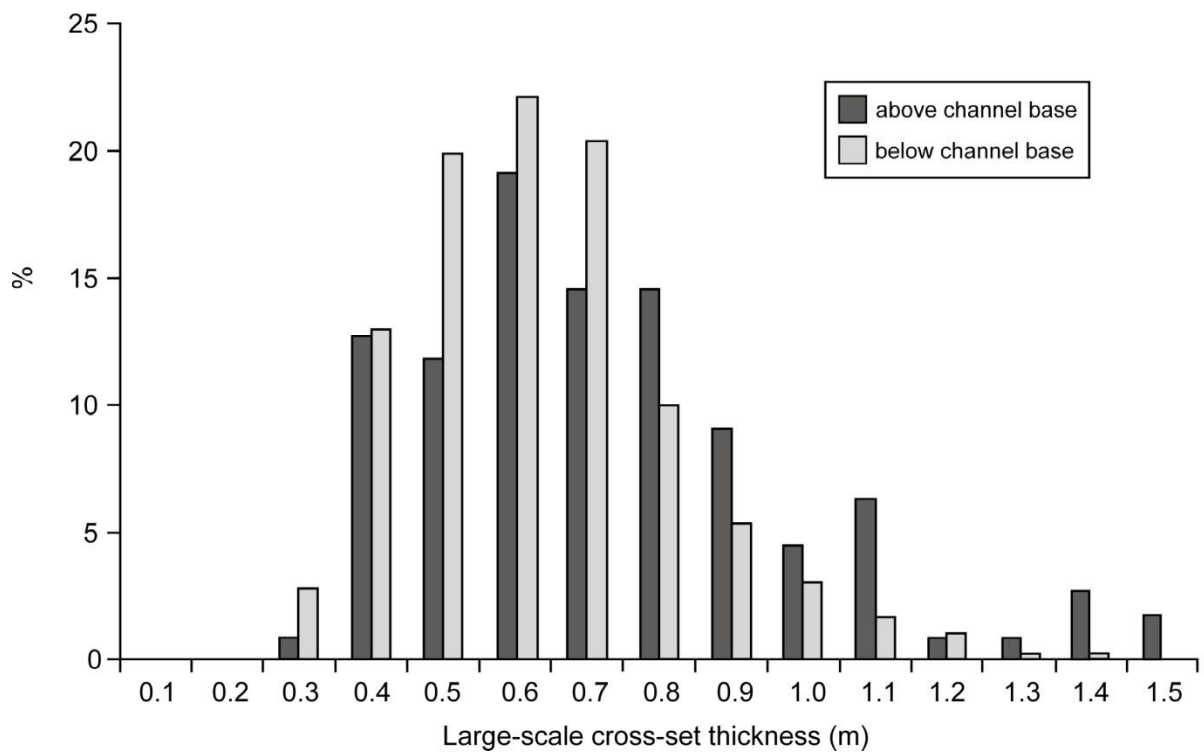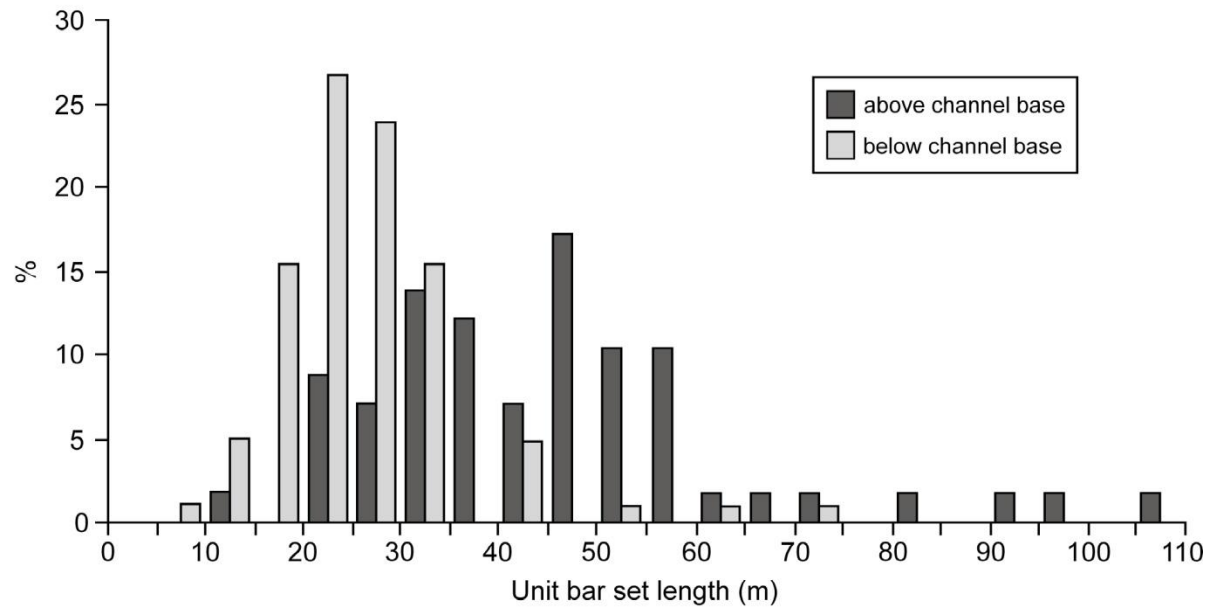
Figure 13: a) Length of large scale cross-sets associated with unit bar deposits as measured from GPR data above (n=110) and below (n=355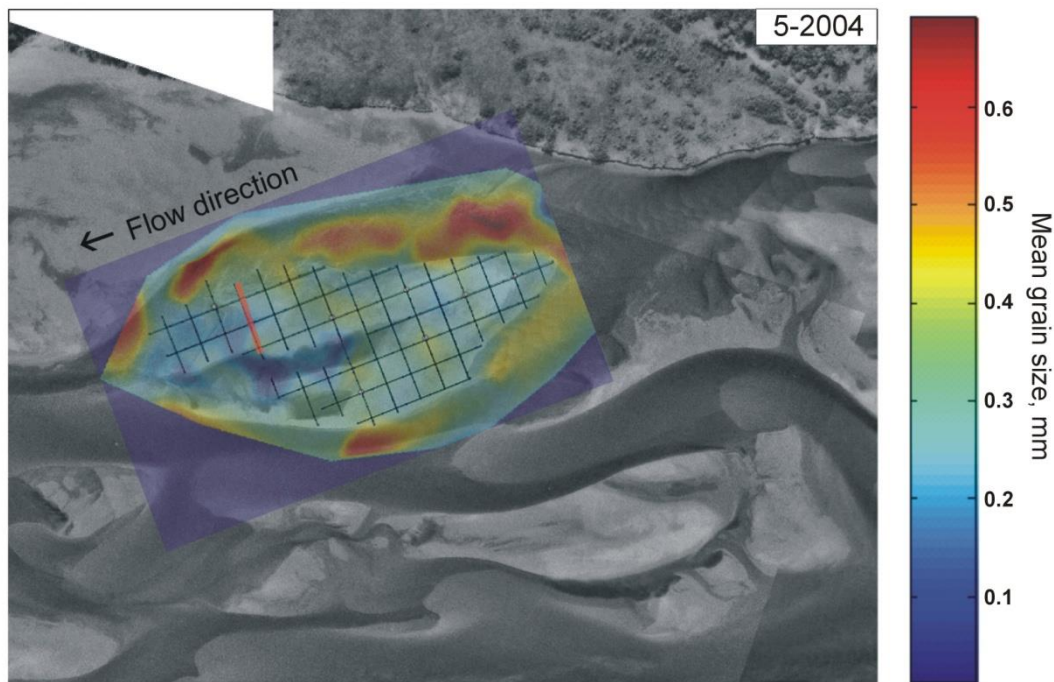) the basal channel erosion surface. b) thickness of large scale cross-sets associated with unit bar deposits as measured from GPR data above (n=110) and below (n=355) the basal channel erosion surface.

Figure 14: Example of surface grain size data collected at Reach B. Note how coarser sediment is found in the channels (red and yellow) around the bar, with the finest sediment located between the bartail limbs (dark blue).
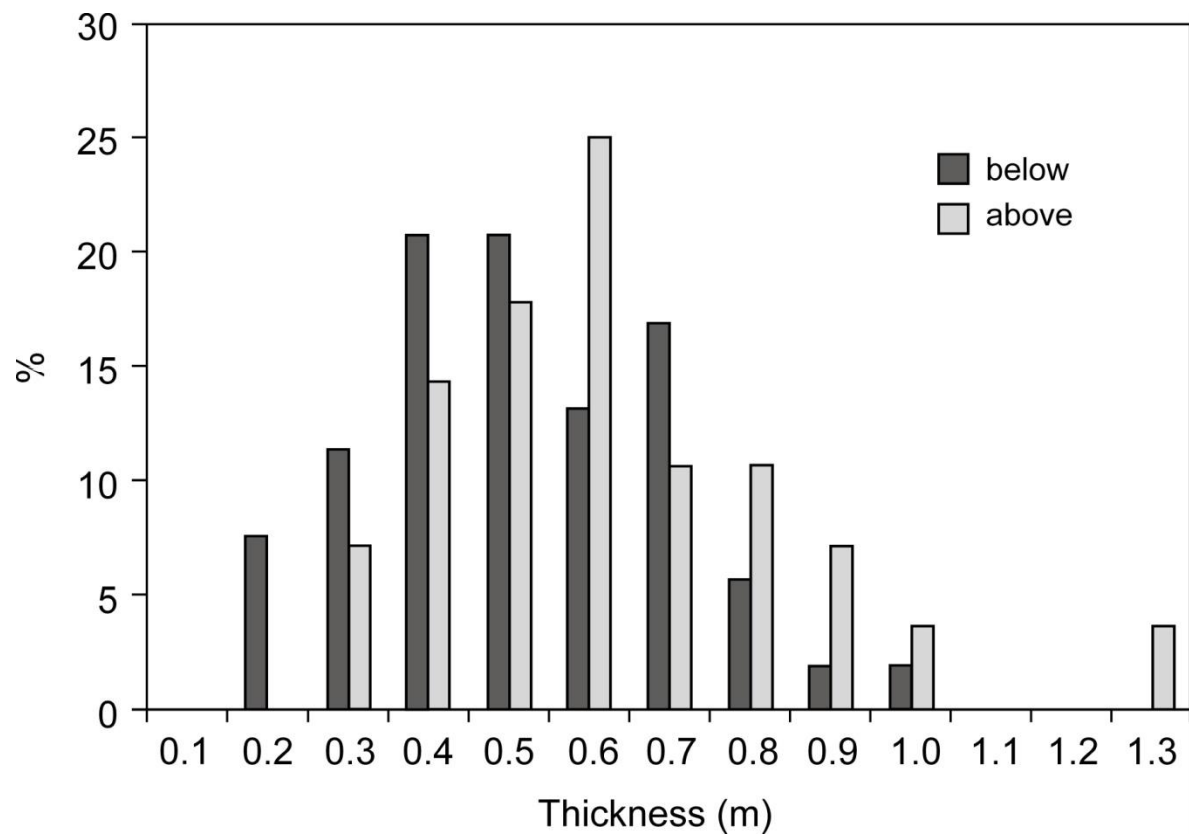
Figure 15: Thickness of cross-sets associated with cross-bar channel deposits as measured from GPR data above (n=28) and below (n=54) the basal channel erosion surface
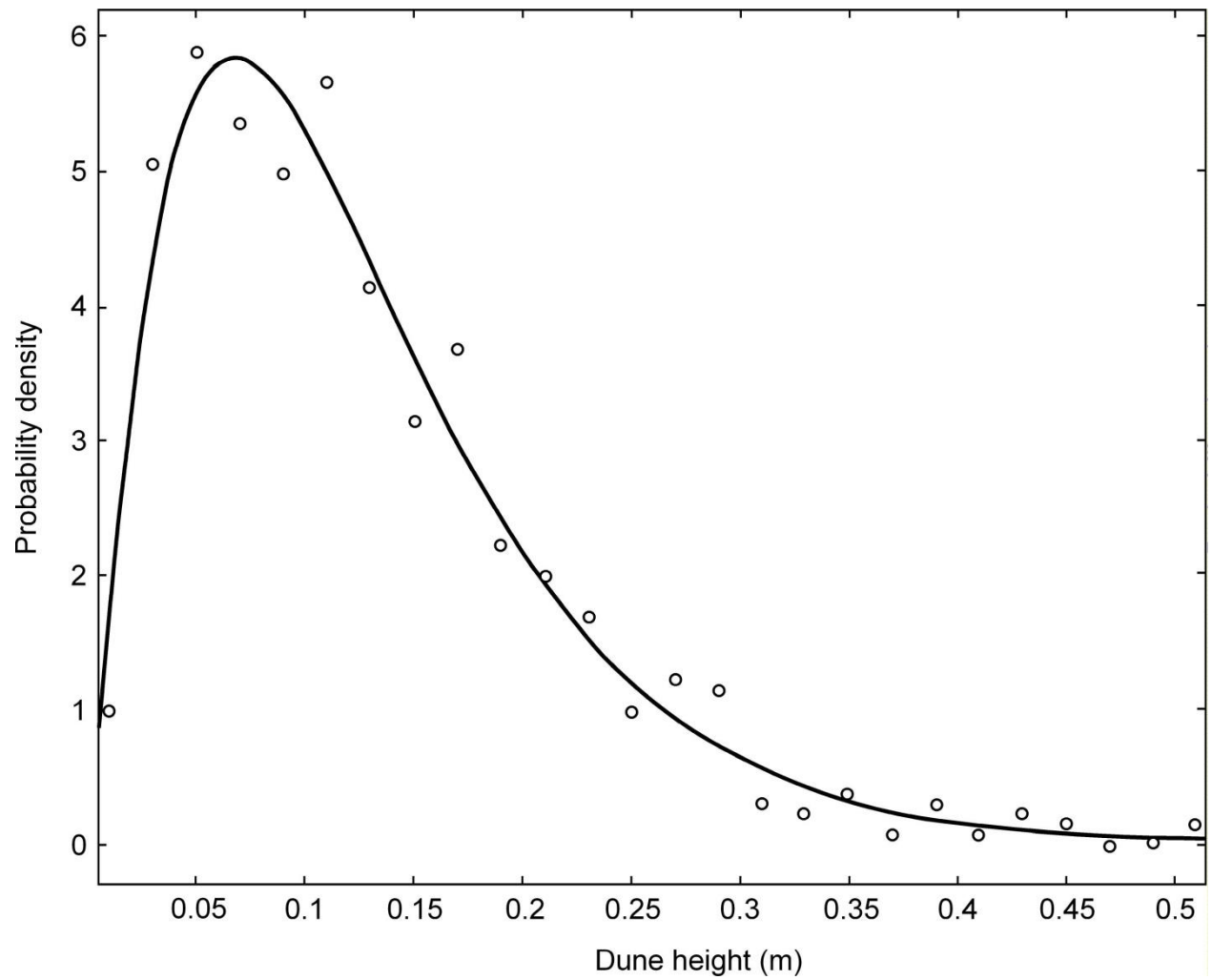
Figure 16: Probability density function of dune height with a two-parameter gamma function fitted according to the method described by Paola and Borgman (1991)